Studies on Effect of Proline Capped Gold Nanoparticles on Hen Egg White Lysozyme (HEWL) and Cytochrome C (Cyt C) Amyloidogenesis

Srijeeb Karmakar

Department of Biotechnology and Medical Engineering
National Institute of Technology, Rourkela

Studies on Effect of Proline Capped Gold Nanoparticles on Hen Egg White Lysozyme (HEWL) and Cytochrome C (Cyt C) Amyloidogenesis

Thesis submitted in partial fulfillment

of the requirements of the degree of

Master of Technology

in

Biotechnology

by

Srijeeb Karmakar

(Roll Number: 215BM2256)

based on research carried out

under the supervision of

Prof. Nandini Sarkar

May 2017

Department of Biotechnology and Medical Engineering

National Institute of Technology, Rourkela

Department of Biotechnology and Medical Engineering
National Institute of Technology Rourkela

Prof. Nandini Sarkar
Assistant Professor

May 24, 2017

Supervisors' Certificate

This is to certify that the work presented in the thesis *Studies on effect of Proline capped Gold Nanoparticles on Hen Egg White Lysozyme (HEWL) and Cytochrome C (Cyt C) Amyloidogenesis*, submitted by *Srijeeb Karmakar*, Roll Number *215BM2256*, is a record of original research carried out by her under my supervision and guidance in partial fulfillment of the requirements of the degree of *Master of Technology* in Biotechnology at *Department of Biotechnology and Medical Engineering of National Institute of Technology Rourkela*. Neither this thesis nor any part of it has been submitted earlier for any degree or diploma to any institute or university in India or abroad.

Prof. Nandini Sarkar
Assistant Professor

Declaration of Originality

I, *Srijeeb Karmakar*, Roll Number *215BM2256* hereby declare that this thesis entitled *Studies on Effect of Proline capped Gold Nanoparticles on Hen Egg White Lysozyme (HEWL) and Cytochrome C (Cyt C) Amyloidogenesis* presents my original work carried out as a M.Tech student of NIT Rourkela and, to the best of my knowledge, contains no material previously published or written by another person, nor any material presented by me for the award of any degree or diploma of NIT Rourkela or any other institution. Any contribution made to this research by others, with whom I have worked at NIT Rourkela or elsewhere, is explicitly acknowledged in the thesis. Works of other authors cited in this dissertation have been duly acknowledged under the section "References". I have also submitted my original research records to the scrutiny committee for evaluation of my thesis.

I am fully aware that in case of any non-compliance detected in future, the Senate of NIT Rourkela may withdraw the degree awarded to me on the basis of the present thesis.

May 24, 2016
NIT Rourkela *Srijeeb Karmakar*

Dedicated to my beloved father,

Late. Sri Jiban Karmakar.

ACKNOWLEDGEMENT

My foremost gratitude is towards **Dr. Nandini Sarkar**, my supervisor, whose valuable guidance and constant help with ideas and resources, opened the avenues for me to learn about a wide range of fields from Nanotechnology, Protein Biochemistry and Computational Biology, applying which I was able to shape my post graduate project to what it is now. I also appreciate her support and help she has rendered me both personally and professionally. I would also like to thank the **Department of Biotechnology and Medical Engineering** for providing me with the opportunity and resources to carry out my study.

I would specially convey my thanks and regards to **Dr. Bibhukalyan P. Nayak, Dr. S.S Ray** and **Dr Mukesh Kumar Gupta**, who not only provided me access to their labs and resources, but also inspired me with their intellectual personality and deep knowledge.

I would express my deepest thankfulness towards my seniors **Tulika Das** and **Rupsa Chatterjee** for their timely help and advices. I am also thankful to **Jagrati Singh, Kanwar Abhay Singh, Geeta Wasupalli,** and **Vidyalatha Kolli** for their co-operation and help in the laboratory. A special mention certainly I wouldn't fail to include is the help I have received from **Praveen Kumar G.** who helped me in my computational work which served me a great deal of assistance.

Finally, I would express all my gratitude towards the Ideal of my life, **Sri Sri Thakur Anukulchandra**, for being the beacon of inspiration in all that I do and achieve, and my mother, **Smt Bina Karmakar**, whose teachings and sacrifice allowed me to become what I am today.

May 24, 2017 Srijeeb Karmakar

NIT Rourkela Roll no- 215BM2256

Abstract

A number of dreadful neurodegenerative diseases like Alzheimer's, Parkinson's and *Amyotrophic lateral sclerosis* (*ALS*) are caused by the culmination of their associated proteins native structure to self-assembled extremely stable fibrils called amyloids. Amyloidogenesis, the process of amyloid formation, is a mechanism still shrouded in mystery. In our present study, we have used the imino acid Proline which is a well known chemical chaperone and is known to interact with Gold colloids, to synthesize Gold Nanoparticles (AuNPs) capped with the same and explore its anti-amyloidogenic ability. The synthesized Proline Capped Gold Nanoparticles (Pro-AuNPs) were vigorously characterized by various techniques like Ultraviolet-Visible (UV) Spectroscopy, Fourier Transform Infra-Red (FTIR) spectroscopy, Dynamic Light Scattering (DLS), Zeta potential measurement and Transmission Electron Microscopy. Our exploration on the anti-amyloidogenic activity of Proline and Pro-AuNPs on two completely unrelated model proteins, namely Hen Egg White Lysozyme (HEWL) and Cytochrome C (Cyt C), unveiled interesting facets to the process. We conclude that irrespective of the evolutionary relationship of all proteins, the process of amyloidogenesis follows a common route driven by a common force. Therefore, it is a great possibility that there might as well be a common inhibitor for all amyloidosis. We also conclude that the effect of inhibition is independent of the charge of the inhibitor and isoelectric point of the protein, rather the chemical structure of the inhibitor is important in the process, which in this case, is the Pyrollidone ring of Proline. We have also seen that conjugation of Proline with AuNPs increases its anti-amyloidogenic tendency by increasing local concentration.

Keywords: Amyloids; Nanoparticles; Proline; inhibition; fluorescene; common mechanism; charge

Contents

Supervisors Certificate ii

Declaration of originality iii

Acknowledgement v

Abstract vi

List of Figures x

List of Tables xii

1.Introduction..... 1

1.1 Introduction.....1

1.2 Objectives.....3

2. Review of Literature.....4

2.1 Protein Folding and Misfolding..... 4

2.2 Anfinson's Dogma and Levinthal paradox 4

2.3 Protein aggregation and amyloidosis.....6

2.4 The process of amyloidogenesis.....8

2.5 Structural characteristics of amyloid fibrils.....9

2.6 Small molecule inhibitors of amyloidogenesis.....10

2.7 Amino acids as inhibitors.....10

2.8 Gold nanoparticles in inhibition of amyloidogenesis.....11

2.9 Imino acid Proline as a chemical chaperone.....12

2.10 Proline interaction with Gold Nanoparticles……...13

2.11 Hen Egg White Lysozyme (HEWL) and Cytochrome C as Model Proteins.....13

3. Materials and Methods.....14

3.1 Reagents and Chemicals.....14

3.2 Synthesis of Proline coated Gold Nanoparticle (Pro-AuNP).....14

3.3 Characterization of Proline Capped Gold nanoparticles (Pro-AuNP).....14

3.3.1 Ultraviolet-Visible (UV) Spectrocopy.....14

3.3.2 Dynamic Light Scattering Size distribution and Zeta Potential measurement.....15

3.3.3 Attenuated Total Reflectance – Fourier Transform Infra Red (ATR-FTIR) Spectroscopy 15

3.3.4 Transmission Electron microscope (TEM) Image.....15

3.4 Inhibition and Disaggregation study.....16

3.4.1 Synthesis of Hen Egg White Lysozyme (HEWL) Amyloids 16

3.4.2 Synthesis of Cytochrome C (Cyt C) Amyloids.....16

3.4.3 Thioflavin T (ThT) Assay.....16

3.4.4 1-Anilinonaphthalene-8-sulfonate (ANS) Assay.....16

3.4.5 Tryptophan Intrinsic Fluorescence Assay.....17

3.4.6 Fluorescence Microscopy.....17

3.4.7 Transmission Electron Microscopy (TEM).....17

3.5 Docking Analysis 18

4 Results and Discussion.....19

4.1 Characterization of Proline Capped Gold Nanoparticles (Pro-AuNPs).....19

4.1.1 Ultraviolet- Visible (UV) Spectroscopy.....19

4.1.2 Particle Size distribution study by Dynamic Light Scattering (DLS).....20

4.1.3 Zeta Potential Distribution study.....21
4.1.4 Fourier Transform Infra-Red (FTIR) Spectroscopic analysis.....22
4.1.5 Transmission Electron Microscopy (TEM).....24
4.1.6 X-Ray Energy Dispersive Spectrometry (EDS).....26
4.1.7 Scanning Transmission Electron Microscopy (STEM).....27
4.1.8 Selected Area Diffraction (SAED) 27
4.2 Synthesis and characterization of Hen Egg White Lysozyme (HEWL) and Cytochrome C (Cyt C) 28
4.3 Inhibition Profiles 29
4.3.1 Thioflavin T Assay.....29
4.3.2 1- Anilinonaphthalene- 8- sulphonic (ANS) Acid Binding Assay.....30
4.3.3 Tryptophan Intrinsic Fluorescence.....32
4.3.4 Fluorescence Microsocopy 32
4.3.5 Transmission Electron Microscopy (TEM).....33
4.4 Computational methods: prediction of amyloidogenic region, binding site of Proline to HEWL and Cyt C & interaction analysis.....35
5. Conclusion.....37
6. Reference.....39

List of Figures

Figure 2.1 Energy Landscape, folding funnel, Anfinson's experiment ……..5

Figure 2.2 Process of amyloid formation ……8

Figure 2.3 High resolution amyloid image, Cross β diffraction pattern ……..9

Figure 2.4 TEM image of amyloid and disaggregation ……...9

Figure 4.1 Absorbance spectrum of Proline Capped Gold nanoparticles ……..19

Figure 4.2 Size Distribution Graph of bAuNPs with Z Average (d.nm) ……20

Figure 4.3 Size distribution graph of Pro-AuNPs with z.average (d.nm) ……...21

Figure 4.4: Zeta Potential of bAuNP ……..22

Figure 4.5. : Zeta Potential of Pro-AuNPs ……..22

Figure 4.6: FTIR spectra of bare Proline, Pro-AuNPs and bAuNPs ……...23

Figure 4.7 High Resolution TEM image of Pro-AuNPs & bAuNPs (after two weeks) ……..24

Figure 4.8 High Resolution TEM image of Pro-AuNPs & bAuNPs (after two months) ……24

Figure 4.9 Size of a bAuNP and Pro-AuNP ……25

Figure 4.10 Lattice fringes of bAuNP and Pro-AuNP ……25

Figure 4.11 Spacing profile of lattice fringes of bAuNPs ……...25

Figure 4.12 Spacing profile of lattice fringes of Pro-AuNPs ……..25

Figure 4.13: EDS Spectrum of bAuNPs ……..26

Figure 4.14: EDS Spectrum of Po-AuNPs ……..26

Figure 4.15: Dark field and STEM image of Pro-AuNPs ……...27

Figure 4.16: SADP of Pro-AuNPs ……..28

Figure 4.17 TEM image of HEWL & Cyt C Amyloids, Small particles observed alongside Cyt C amyloids, EDS of the small particles ……29

Figure 4.18 Thioflavin T assay of HEWL and Cyt C: inhibition study ……..30

Figure 4.19 (ANS)fluorescence vs. time curve for HEWL & Cyt C ……..31

Figure 4.20 Tryptophan intrinsic assay ……...32

Figure 4.21 Fluorescence Microscopy images of HEWL ……...33

Figure 4.22 TEM images of HEWL amyloids: Inhibition and Disaggregation ……..34

Figure 2.23 TEM images of Cyt C Amyloids: Inhibition and Disaggregation ……...34

Figure 4.24 HEWL: FoldAmyloid, LIGPLOT, Chimera view of docking …….35

Figure 4.25 Cyt C : FoldAmyloid, LIGPLOT, Chimera view of docking ……..36

List of Tables

2.1 List of amyloidosis associated to the aggregation of several proteins ……6

4.1 List of size distribution Results obtained from DLS for bAuNPs ……..20

4.2 List of size distribution Results obtained from DLS for Pro-AuNPs ……21

Chapter 1

Introduction

1.1 Introduction

Amyloidogenesis is the transition of a protein to an organized self-assembled misfolded structure called amyloid, which otherwise at normality would have attained a three dimensional native structure in accordance to its specific function. The mechanism, although is under a great deal of research, is still shrouded in mystery. Amyloidogenesis is the root agent for several dreadful neurodegenerative diseases like Alzheimer's, Parkinson's and *Amyotrophic lateral sclerosis (ALS).* As a proteins structure is of utmost importance for its function, the misfolded proteins lose their function, rather form extremely stable fibrils, deposit in cells and block cellular transport.

Protein folding to its native structure is thermodynamically driven, but if the thermodynamic favourability is for a misfolded conformation, cells have specialized proteins called chaperones, which as the name suggests, guide the process of folding towards the nativity. With age, however, the expression of the chaperones decreases resulting in the formation of misfolded aggregates of proteins rather than functionally active structures. These aggregates self-assemble and organize themselves into anti-parallel beta sheets to ultimately form amyloids.

Amyloidogenesis is driven by hydrophobic interactions with which the unfolded or misfolded structure aggregate. The hydrophobic residues of a protein are normally embedded at the core which gets exposed when the protein unfolds. Therefore, there are distinct stages of amyloidogenesis, which commences with aggregation at first. The aggregates form ordered structures called oligomers which assemble by hydrophobic interaction. Finally upon reaching a critical nucleation point, extremely stable at low energy levels fibrillar structures are formed, rich in cross β sheet, which are called the amyloids. Mathematically, the three stages have a pattern of a sigmoidal curve.

Several proteins, recognized over twenty, are known to be prone to amyloidogenesis and are associated to severe health problems. Although, they share no or little structural similarity or amino acid sequence, the amyloids form have a common structure which is the paradox of the

problem. There has been a great deal of research to not only understand the mechanism but also find inhibitors which would prevent amyloidogenesis to take place.

In our study, we have chosen Hen Egg White Lysozyme (HEWL) and Cytochrome C (Cyt C) as model proteins. Our utmost objective was to find an insight into the mechanism of action of amyloidogenesis by comparing two unrelated proteins. HEWL is a readily available and affordable protein, sharing structural similarity to its human analogue, Lysozyme, whose amyloidogenesis is associated to Hereditary non-neuropathic systemic amyloidosis. Secondly, Cytochrome C is an interesting protein to study for its highly alpha-helical structure, its prosthetic group heme, and its function in electron ransport chain, all that makes it very different from HEWL.

As an inhibitor, we have selected proline from the 20 amino acids as it has been reported as a chemical chaperone during experiments involving protein folding. Proline is also hydrophobic for which our investigation into the role of hydrophobic interaction in the entire process finds a new avenue. Moreover, Proline is known to interact with the Gold colloids, which served our yet another crucial objective to use Gold nanoparticles as specialized agents for delivery of the inhibitors. The effect of Gold nanoparticles towards the conjugated molecules with potential inhibitory ability has been previously found to increase by many folds.

We have used several chemical and biophysical techniques to synthesize and characterize Gold nanoparticles capped with proline like UV-Vis spectroscopy, Dynamic Light Scattering (DLS) and Zeta potential measurement, Fourier Transform Infre-Red Spectroscopy (FTIR), Transmission Electron Microscopy etc. To investigate its effect on the amyloidogenesis of HEWL and Cyt C we have performed several Flurescence assays like Thioflavin T assay, ANS dye binding assay, Tryptophan intrinsic assay, flurescence microscopy etc. TEM images finally were taken to validate the results visually and to understand the chemistry of the interactions, computational methods were used to dock Proline with the proteins and predict the interaction using LIGPLOT.

1.2 Objectives

1) Synthesis of Proline capped Gold nanoparticles.
2) Characterization of synthesized gold nanoparticles utilizing several biophysical techniques like UV-Vis Spectroscopy, DLS and Zeta potential measurement, FTIR, TEM etc.
3) Studying effect of Proline Capped Gold nanoparticles on HEWL and Cyt C amyloidogenesis.
4) Understanding the mechanism of action of the synthesized nanoparticles through various biophysical, microscopic and computational analysis

Chapter 2

Review of Literature

2.1 Protein Folding and Misfolding

The mechanism and various factors involved in protein folding and misfolding has been discussed in detail by Dobson *et al*. It has been stated that the manner in which a protein folds into its native structure depends on the intrinsic properties of its amino acid sequence and other contributing factors from the crowded cellular environment [1]. Protein folding is explained in terms of entropy which is the degree of randomness or freedom of a polypeptide coming out from the ribosome. As the protein folds the entropy decreases and the native structure is formed in a low energy state [2,3,4] (Figure 2.1a & Figure 2.1b)

The bonds involved are disulphide bonds, hydrogen bonds, hydrophobic interaction and ionic interaction [1,5]. If the native structure is not thermodynamically favorable or in order to screen the influences of other interactions in the process, molecular chaperons guide proteins to their proper folded state [8].

The best characterized of the chaperones studied in this manner is the bacterial complex involving GroEL, a member of the family of 'chaperonins', and its 'co-chaperone' GroES. With age, expressions of these chaperones decrease which results in protein misfolds [9].

When protein escape the quality control checks it misfolds and forms amyloids which are extremely stable structure owing to their very low energy level. The primary interaction in amyloids is hydrophobic and hydrogen bonding. Amyloids, irrespective of their origin, exhibit a similar structure which is cross-beta sheets. Aggregation of misfolded proteins that escape the cellular quality-control mechanisms is a common feature of a wide range of highly debilitating and increasingly prevalent diseases [10].

2.2 Anfinson's Dogma and Levinthal Paradox

Christian B. Anfinson (Nobel Prize in chemistry, 1972) stated, following his observations with the folding of Ribonuclease A, that the folding of a polypeptide to its native conformation is determined by the intrinsic sequence of its amino acids, at least for small globular proteins. The postulate says that the environmental conditions (temperature,

composition and solvent concentration) at which the folding of a protein takes place, the native structure therein is stable, unique and kinetically at its minimum energy [11,12].

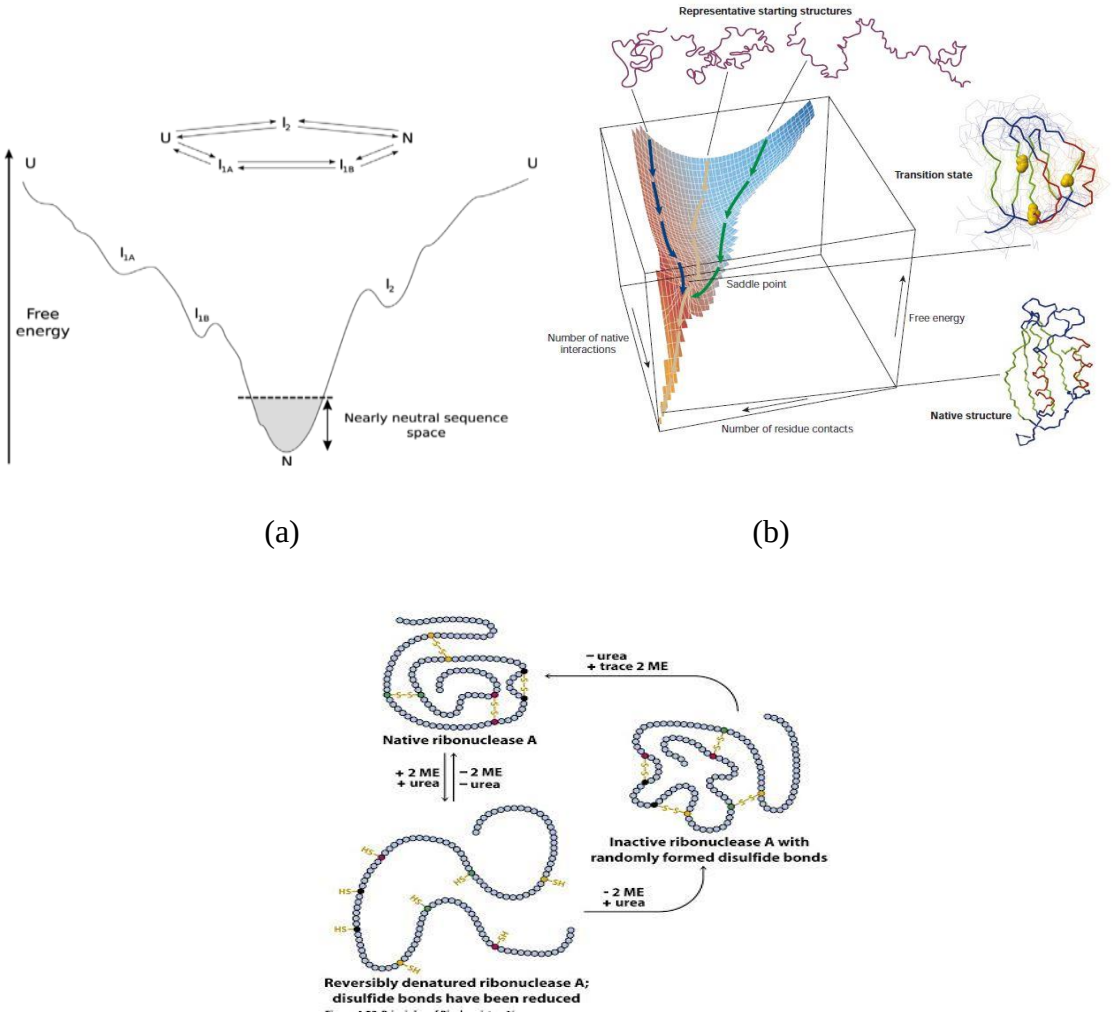

Figure 2.1. (a) Schematic representation of the folding funnel showing two alternative folding pathways which a protein would take to reach its native conformation (N) from its unfolded state (U) either through (I_2) or (I_{1A} and I_{1b}). (b) Landscape of Folding funnel showing rapid folding of a protein from to its native state by attaining several metastable intermediate states. (c) Schematic representation of the Anfinson's experiment.

Conversely, Cyrus Levinthal stated following his thought experiment (figure 2.1c) that if a polypeptide is kinetically driven to randomly search for its most favorable conformation then it would take an astronomical amount of time for it attain a native conformation. For example, if a polypeptide is a 100 residue long, it has 99 peptide bonds, 198 different psi and phi bonds, owing to which the degree of freedom is so large that the number of possible

conformations a polypeptide would randomly search was estimated to be 3^{300} or 10^{143} . But Levinthal was aware that a polypeptide folds in milliseconds or even faster. He suggested that the paradox could be resolved if the folding of a polypeptide is guided by rapid local interactions of the amino acids which serve as nucleation points for the folding to take place, thus speeding up the process by reducing number of possible conformation. The notion of intermediates in protein folding and partially folded states called transition states, was validated experimentally and thus, it provided evidence for the fast protein folding process. Moreover, Levinthal also suggested that the native structure of a protein is at a higher energy level than the minimum energy it could attain, which explains why proteins are prone to degradation. Edward Trifonov and Igor Berezovsky suggested that a polypeptide folds in units or modules of 25-30 amino acids [13,14,15]

2.3 Protein aggregation and amyloidosis

Essential proteins which have crucial functions in the physiological system sometimes aggregate after escaping from the quality control mechanism and causes a group of protein conformational disorders called amyloidosis [1] Table 2.1 provides a list of diseases which are caused by the fibrillation of specific proteins specific to diseases.

Table 2.1: List of amyloidosis associated to the aggregation of several proteins

Amyloidosis	Featured Protein	Official abbreviation
Alzheimer's disease	Beta-amyloid from Amyloid precursor protein	Aβ, APP
Parkinson's disease	Alpha-synuclein	None
Fatal familial insomnia	PrPsc	APrP
Medullary carcinoma of the thyroid	Calcitonin	ACal
Atherosclerosis	Apolipoprotein AI	AApoA1
Aortic medial amyloid	Medin	AMed
Familial amyloid polyneuropathy	Transthyretin	ATTR
Dialysis related amyloidosis	Beta-2 microglobulin	Aβ2M
Lattice corneal dystrophy	Keratoepithelin	Aker

Cerebral amyloid angiopathy (Icelandic type)	Cystatin	ACys
Sporadic Inclusion body myositis	S-IBM	None
Diabetes mellitus type 2	IAPP (Amylin)	AIAPP
Transmissible spongiform encephalopathy	PrPsc	APrP
Huntington's disease	Huntingtin	None
Cardiac arrhythmias, isolated atrial amyloidosis	Atrial natriuretic factor	AANF
Rheumatoid arthritis	Serum amyloid A	AA
Prolactinomas	Prolactin	APro
Finnish amyloidosis	Gelsolin	AGel
Cerebral amyloid angiopathy	Beta Amyloid	Aβ
Systemic AL amyloidosis	Immunoglobulin light chain AL	AL
Hereditary non-neuropathic systemic amyloidosis	Lysozyme	ALys

The process by which proteins misfold is similar in pattern to that of crystallization wherein the formation of nucleus is a must. The process appears to onset when partially folded up conformations facilitate such intermolecular interactions, predominantly hydrophobic and hydrogen bonding, that at first oligomeric misfolded structures are formed, then the process is driven towards polymerization into amyloid fibrils. This is known as the polymerization hypothesis [16,17].

In yet another hypothesis is called the conformational hypothesis which postulates that amyloid formation takes place by the conformational changes of the protein and misfolded conformations may or may not aggregate [17]

In intermediate view hypothesis, it is postulated that the partially folded or misfolded structures of a protein might expose the hydrophobic patches which interact among each other and stabilizes, leading to the formation of β sheet oligomers. These oligomers themselves interact to form fibrillar structures of the protein called amyloids [17].

2.4 The process of amyloidogenesis

The process of amyloidogenesis (Figure 2.2a), i,e, formation of amyloid fibrils, is representated by a sigmoidal curve which has distinct phases, namely- Lag, Exponential and saturation phases (figure 2.2b). The first stage of the amylidogenesis is the occurrence of bead-like oligomers (also called prefibriilar aggregates) rich in β sheet assembled from soluble monomers. It is followed by a rapid logarithmic or exponential phase, wherein, the oligomers arrange themselves in short, fine, curly structures called protofibrils. To the end of preformed β sheet soluble species in ^{turn} arrange themselves, leading to the elongation of β sheet. Another route is lateral addition where the soluble species add the β sheet to their side. The protofibrils then organize themselves into extremely stable, continuous mature fibrils in, what is called as the saturation phase. Therefore, a transition of soluble monomer to insoluble fibril rich in β sheet and their deposition at various sites of the body is the overall driving force towards the formation and pathology associated to amyloid fibrils [1,18]

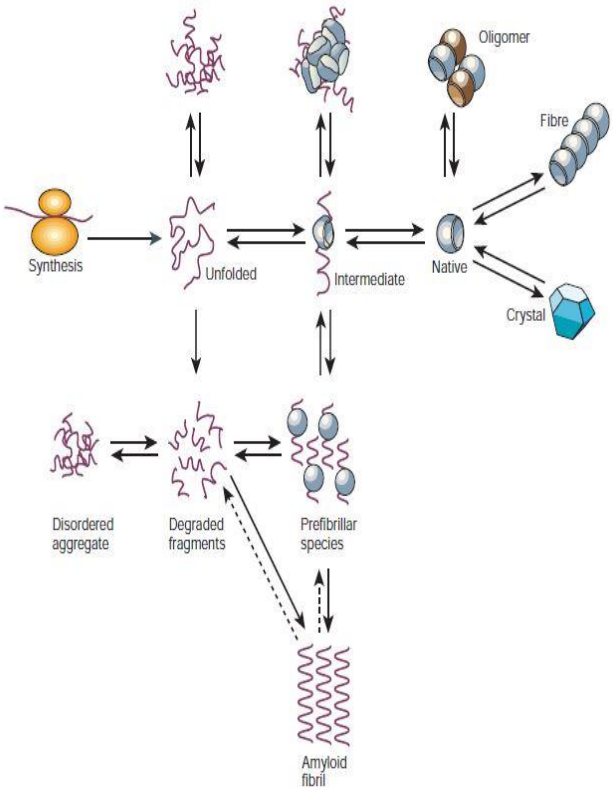

Figure 2.2 (a) Schematic diagram showing several states a protein molecule can culminate into. As a protein molecule is synthesized, it can reach its native structure through several intermediates states. But it can also culminate into other fates like degradation and aggregation. The difference between other aggregates and amyloids lies in attaining ordered geometrical structures. Amyloids have an organized self-assembled misfolded structure rich in anti parallel Beta sheets

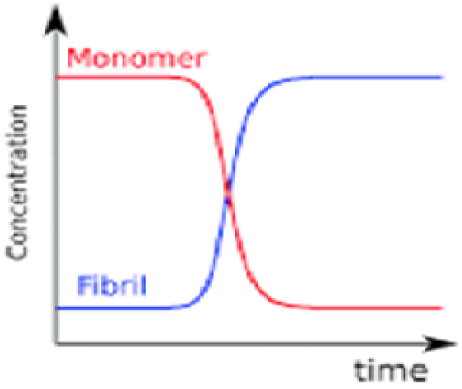

Figure 2.2 (b) Graph showing the concentration of fibrils increasing with time alongside the decreasing concentration of monomeric form of the protein.

2.5 Structural characteristics of amyloid fibrils

The structure of the amyloid fibrils has been determined mostly by X-Ray Diffraction and techniques involving electron microscopy [19]. Eletroparamagnetic resonance [20]and solid state nuclear magnetic resonance (ssNMR) [21] are among the most recent techniques which have been applied to determine the structure of amyloids. Revealed by several of these techniques, Amyloids are composed of unbranched, straight and long structures, and polymers of structural units called the protofilaments [22]. ssNMR studies have revealed, as in the case of Aβ protein, that the fibrils might be formed of parallel or antiparallel arrangement of β sheet [23]. The cross β diffraction fingerprint found in the X-ray diffraction technique is indicative of the fact that the amyloids are rich and are composed in their core structure with β sheet [24]

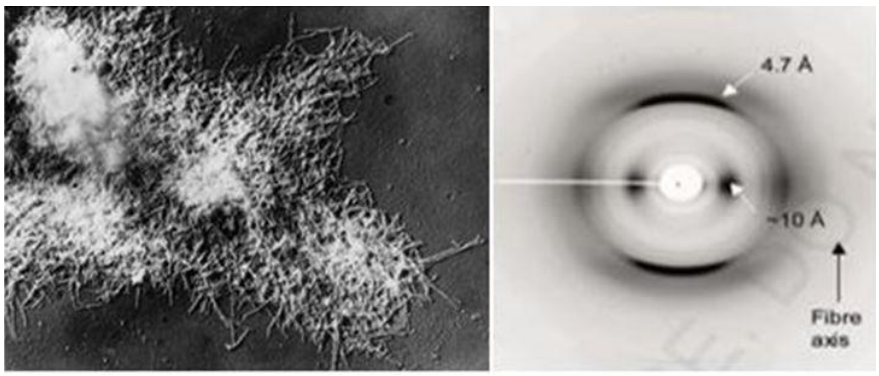

(a) (b)

Figure 2.3 (a) Amyloid fibrils obtained from amyloidotic spleen of humans (b) cross β" Diffraction pattern of amyloids.

2.6 Small molecule inhibitors of amyloidogenesis

Molecules small enough to penetrate into the Beta sheets and destabilize the hydrogen bonds of the fibril core and the hydrophobic interactions between amino acid side chains, have been used to investigate disaggregation of the human lysozyme. The compounds chosen consist of a single hydrophobic benzene ring di- or trisubstituted with potential hydrogen bond donors or acceptors. Out of 20 compounds already studied with the beta amyloid peptide, 5 were selected for the study, they are 3,4-dihydroxybenzoic acid (3,4DHB), 2- hydroxy-3- ethoxybenzaldehyde (2H3EB), 4-aminophenol (4AP), 4-aminoanisole (4AA), and 2-amino-4-chlorophenol (2A4CP). Disaggreagation was followed by ThT fluroscence measurements. 4-AP and 2A4CP efficiently inhibit the aggregation and disrupt amyloid fibrils from hen and human lysozymes. [25]

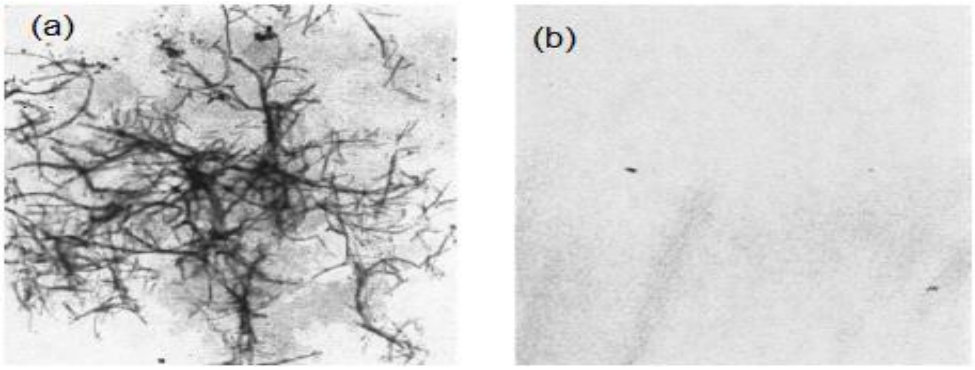

Figure 2.4(a) Transmission Electron Microscopic image of Amyloid of Hen Egg White Lysozyme. (b) Disaggregation of amyloids using 4-AP.

2.7 Amino acids as inhibitors

Amino acids offer a great range of interactions including hygrogen, hydrophobic, ionic and covalent interactions [26]. The molecules must interact with the residues at the amyloidogenic region of the protein.

L-arginine has been reported as a renaturant of already misfolded proteins. Hen egg white lysozyme was used as a model protein to study the inhibition process. By chemically modifying the cysteine residues in the amino acid back bone chain, several unfolded species of the protein were obtained, each treated with L-arginine as a renaturant. The amino acid was found to increase the equilibrium solubility of the unfolded states and intermediates, resulting in renaturation [27].

Amyloid Beta protein amyloidogenesis has been reported to be inhibited by quenching the nucleation and elongation phases of the aggregation process by involving a low concentration of chemically modified cysteine, N-acetyl cysteine, and conjugating with quantum dots. a 100 fold increase in the concentration of the functionalized quantum inhibit the process remarkably. It is suggested that the mechanism of inhibition is by interaction of the N-acetyl cysteine with the amyloid fibrils by hydrogen bonding and blocking the elongation phase therbeby [28]. Another report on the inhibition of Tau protein aggregation associated with Alzheimer's disease by D-amino acids and a non-natural amino acid which is involved in the enhancement of sexual transmission of HIV [29]. Inhibition of Amyloid beta protein aggregation associated with the same disease has also been reported by the involvement of chemically modified amino acids at alternate residues of small peptides. Chemical modification was done by N-acetylation [30].Gluthathione, a tripeptide, has been reported to be an efficient inhibitor of Lysozyme amyloidogenesis which was added within 6 days of incubation. SDS-PAGE results has shown that the addition of Gluthathione led to lysozyme hydrolysis prominently. It has been suggested by the redox environment plays an important role in the fibrillation process [31].Aromatic amino acids, Tyrosine and tryptophan, has shown inhibition of insulin fibrillation. Aggregation was induced by both spontaneous and seed-induced methods. It has been proposed that inhibition was brought by the interaction of the aromatic amino acids with the protein by its aromatic moiety, carbonyl and amino group. Further, conjugation of these amino acids with gold nanoparticle increases their anti-amyloidogenic propensity [32].

2.8 Gold nanoparticles in inhibition of amyloidogenesis

Gold Nanoparticles conjugated with various organic and biomolecules exhibits biocompatibility, owing to which, the importance of the same in the material science has attracted much attention as a therapeutic agent [33]. Physicochemical characteristics like charge and hydrophobicity of the Gold nanoparticles can be altered by surface modification thus offering a wide range of biological applications ranging from labelling to delivery [34,35,36]. The interaction of gold nanoparticles with proteins adsorbed onto the surface can bring about conformational changes in the three dimensional structure of the protein [37]. The aggregation growth rate of α-synuclein, a presynaptic protein associated with parkinson's disease, has been observed to delay in the influence citrate capped gold nanoparticles [38]. Also, amino acids exert a biophysical inhibiting effect on the aggregation of proteins [39].

Amino acids serve as efficient reducing agents in the synthesis of Gold nanoparticles and also capping molecules to increase stability. The chemistry is that amino acids can reduce gold ions to neutral gold by their amino group as reported in the synthesis of tryptophan reduced and tryptophan capped Gold nanoparticles [40]. Various strategic synthesis of gold nanparticles functionalized with amino acids has been reported involving various interactions like electrostatic attraction and covalent/coordinate bonding with arginine and aspartic acid [41]. Glutamic acid reduced carboxylated gold nanoparticles have been found to be stable and monodispersed, alongside exerting an effect in the secondary structure of BSA and IgG proteins [42]. Tryptophan and tyrosine coated gold nanoparticles inhibited the spontaneous and seed induced aggregation of insulin, wherein, bare tryptophan and tyrosine did not inhibit the aggregation at all unless until was conjugated to gold nanoparticles [32]. Gold nanoparticles capped with glycine, aspartate, leucine, lysine and serine have shown considerable effect on the absorption and cytoxicity of serum albumin [43].

2.9 Imino acid Proline as a chemical chaperone

Proline as an osmolyte among many has shown inhibitory effect in aggregation during refolding of HEWL. Experimental evidence suggests that proline binds with folding intermediates and traps the intermediates into ‘aggregation insensitive’ state, which are enzymatically inactive. The inhibitory effect was attributed to the ability of proline to form supramolecular amphipathic higher order aggregates and provide osmoregulation under water stress [44]. Proline acts as chemical chaperone stimulating the renaturation of citrate synthase after urea denaturation and also inhibits its thermo-denaturation [45]. Proline has also been featured as a protein compatible hydrotrope, which self aggregates and assembles noncovalently providing a microenvironment with lowered polarity decreasing the hydrophobicity of the system [46]. Proline increases the solubility of proteins attributing to the self assembly into higher order aggregates [47]. In yet another study, Proline and sorbitol, were found to be effective in the inhibition of insulin and lysozyme wherein both the compounds established polar interaction during the elongation and saturation stages of fibrillation comparing to the native state. Presence of hydrophobic interactions is also suggested [48]. Moreover, proline is also a potent breaker of beta sheet which is found predominantly in the amyloid fibrils. Adding up to its attractive features, proline also protects alpha helix and helps in retaining its intactness [49]. In another study, the structural implication of presence of proline in particular sites towards the amyloidogenic propensity of

the Islet amyloid polypeptide (IAPP) was conducted. It has been demonstrated that substituting proline with amino acids in the amyloidogenic region of Islet amyloid polypeptide (IAPP) results in substantial inhibition of amyloid formation [50].

2.10 Proline interaction with Gold nanoparticles

Proline can also interact with Gold nanoparticles by its amino and carboxyl moieties. It appears to form an anchor bond N-Au or O-Au with associated hydrogen bonding between hydroxyl group and Au (OH....Au). Among the possible interaction, it appears that the tendency of interaction between the amide group and Au is higher. The results were substantiated by Natural Bond orbital analysis (NBO) [51].Thus, the various lucrative characteristics of proline as a potential inhibitor and its ability to interact with gold nanoparticles has led us to synthesize proline capped gold nanopaticles and investigate the inhibitory effect on completely unrelated proteins to understand the influence of charge, isoelectric points of proteins in the mechanism of fibrillation and in the process, understand the mechanism of amyloidogenesis of proteins which is yet shrouded in mystery.

2.11 Hen Egg White Lysozyme (HEWL) and Cytochrome C as Model Proteins

HEWL is a 129 a.a (amino acid) long enzyme whose function lies in the lysis of bacterial cells walls. It is generally considered a model protein for amyoid inhibition studies. The reasons for it to be a good model protein is that it is affordable and easily available. Also it is well characterized, forms amyloids easily *in vitro* and shares structural similarity to its human analogue, lysozyme (almost 60%) which is responsible in causing hereditary non neuropathic systemic amyloidosis in humans after it misfolds and deposits in liver and kidneys [52].

Cytochrome C, a completely unrelated protein to that of HEWL, forms amyloids in a very interesting way. The heme group at the core of the holo protein stabilizes the structure. However, in amyoidogenic conditions, the loss of the heme group results in misfolding of the protein and formation of straight, amyloid structures. The salient feature is that even though the protein is highly α-helical it still forms the most common β-sheet rich structures associated with typical protein aggregates [53].

Chapter 3

Materials and Methods

3.1 Reagents and Chemicals

Gold (III) Chloride hydrate, Thioflavin T, Hen eggwhite lysozyme, Cytochrome C and 1-anilinonaphthalene -8-sulfonate (ANS) were purchased from Sigma-Aldrich (Kolkata, West Bengal, India). L-proline and Tri-sodium citrate were purchased from Himedia (Mumbai, Maharashtra, India). All other chemicals were of analytical grade.

3.2 Synthesis of Proline coated Gold Nanoparticle (Pro-AuNP)

Gold nanoparticles were synthesized using the well known Turkevich method, wherein, 200 microlitres of 2% Gold (III) Chloride solution was added to 50 mL boiling distilled water kept on the magnetic stirrer. It was followed by addition of 0.05M Tri-Sodium Citrate to the solution. The culmination of the reaction is confirmed by the appearance of deep ruby red colour with 40 ppm concentration of negatively charged Gold nanoparticle [54,55]. A part of the solution was kept as bare gold nanoparticle (bAuNP). L-Proline dissolved in acetate buffer maintained at acidic pH below the pI value of Proline (pI-6.3) at which it attains positive charge was added to the synthesized Gold nanoparticles in 10-fold excess concentration but 10-fold lesser volume. The driving force behind the interaction of the amino acid and the gold nanoparticle surface is electrostatic chemisorption i,e, the amino acid is adsorbed on the surface of the gold nanoparticle by electrostatic forces [56].

3.3 Characterization of Proline Capped Gold nanoparticles (Pro-AuNP)

3.3.1 Ultraviolet-Visible (UV) Spectrocopy.

The synthesized nanoparticles (bAuNP and Pro-AuNP) were characterized by analyzing their spectroscopic absorption of visible light in the wavelength range from 400-700nm with a scanning speed of 350nm/min, in Perkin Elmer UV-Vis Spectrophotometer, Lambda-19. A

blank reference was scanned for correcting the baseline screening the absorption of the dispersant and other molecules. The analysis and recording of the data was done by "UVWinlab" software integrated in the instrument.

3.3.2 Dynamic Light Scattering Size distribution and Zeta Potential measurement

Zeta Sizer Nano-ZS (Malvern instrument, UK) was used to measure the hydrodynamic diameter of both the bAuNP and Pro-AuNP for comparative analysis. The measurements were taken in Automatic mode. The stability and charge of the nanoparticles were analyzed by measuring the Zeta potential of the particles using a Zeta Sizer Nano-ZS (Malvern Instruments, UK).

3.3.3 Attenuated Total Reflectance – Fourier Transform Infra Red (ATR-FTIR) Spectroscopy

To understand the spectral characteristics and thereby confirming the capping of Proline to the surface of Gold nanoparticles, FTIR spectroscopic analysis was done in ATR mode. To screen the influence of the dispersant a blank reference was used. The measurement was done within the wavenumber range of 0-4000 cm^{-1}. For comparative analysis, FTIR spectroscopy was performed for bAuNP, bare Proline and Pro-AuNP.

3.3.4 Transmission Electron microscope (TEM) Image

The shape, size, crystallinity and the morphology of the synthesized AuNPs was investigated in TEM in various modes- conventional Transmission Electron microscopy (cTEM), Scanning Transmission Electron Microscopy (STEM), selected Area Diffraction (SAED), and Energy Dispersive X-Ray spectroscopy (EDS). Both dark field and bright field images were obtained. The sample preparation of AuNPs was done by placing a carbon coated TEM copper grid on a fine tissue paper and then, 10 µL of AuNPs solution was dropped on the grid in the drop-casting methodology. Excess solution was removed by the capillary action of the tissue paper. The sample was desiccated for a prolong time for complete drying.

3.4 Inhibition and Disaggregation study

3.4.1 Synthesis of Hen Egg White Lysozyme (HEWL) Amyloids

The lysozyme amyloidosis was induced by incubating 35 μM HEWL in 10mM Glycine-Hydrochloride (Gly-HCL) buffer maintained at pH 2, at 55 °C and 30 rpm. The HEWL [4]. In order to investigate the inhibition of amyloidosis by proline, 20-fold molar excess proline but 1% of the total volume, was incubated alongside HEWL under the same amyloidogenic condition. Pro-AuNP was incubated similarly with HEWL but the volume of solution used was 100 μL. Disaggregation study was performed by incubating preformed mature fibrils with Proline and Pro-AuNP at 37°C overnight [57].

3.4.2 Synthesis of Cytochrome C (Cyt C) Amyloids

The amyloidosis of Cyt C was induced by incubating it in 90μM concentration in 10mM Tris-HCL buffer maintained at pH 9 and temperature 75°C. Proline and Pro-AuNP were also individually incubated alongside Cyt C under the same amyloidogenic conditions. For disaggregation study, the preformed amyloid fibrils were incubated with Proline and Pro-AuNP individually at 37°C overnight [58].

3.4.3 Thioflavin T (ThT) Assay

ThT Stock solution was prepared by dissolving appropriate amount of ThT in 10mM Phosphate buffer (pH-6.5) to make 2.5mM concentrated solution and then, stored in dark for its light sensitiveness [59]. Aliquots were drawn from incubated HEWL and Cyt C, alongside the test samples incubated with Proline and Pro-AuNP, in a time dependent manner until 96 hours. The sample preparation was done by adding 857 μL of the incubated protein samples with 30 μL of ThT to make a final volume of 3000 μL. The samples were incubated in dark for half an hour. Fluorescence measurements were taken in Fluromax 4 (Indian Institute of Technology Guwahati) with emission scan range 460-610 nm and excitation at 450nm. Slit width during the measurement was kept at 5 nm both for excitation and emission. The final analysis of the data was done by subtracting the blank reference.

3.4.4 1-Anilinonaphthalene-8-sulfonate (ANS) Assay

ANS assay was performed to investigate the state of hydrophobic surfaces of the protein during amyloidosis incubated with and without Proline and Pro-AuNPs. Similar to ThT

assay, a time dependent study was done for the same. ANS stock solution was prepared freshly by dissolving appropriate amount of the dye to maintain 2.5 mM concentration in 0.5mL methanol at first, followed by dissolving the same in 9.5 mL distilled water. The sample preparation was done in such a way to maintain the ANS concentration in 100 fold molar excess to that of HEWL and Cyt C. The samples were incubated in dark for half an hour. Measurements were taken in Fluromax 4 (Indian Institute of Technology, Guwahati) with emission scan range 390- 600 nm and excitation at 380nm. Slit width for both excitation and emission was maintained at 5nm. The final analysis of the data was done by subtracting the blank reference [60].

3.4.5 Tryptophan Intrinsic Fluorescence Assay.

HEWL and Cyt C were incubated with and without proline and Pro-AuNPs. Aliquots were drawn at 24, 48 and 72 hours. The sample was prepared by maintaining the final concentration of protein to be 5μM at pH 2 and 9 for HEWL and Cyt C respectively. The measurement was taken by selectively exciting the sample for Trytophan fluorescence at 295 nm and scanning for emission was taken in the range 300- 450 nm.

3.4.6 Fluorescence Microscopy

Fluorescence microscopy samples were prepared by placing 5μL of HEWL and Cyt C incubated with and without Proline and Pro-AuNPs, on a glass slide and adding 10 μL of 1mM ThT stock solution prepared by dissolving appropriate amount of ThT in Phosphate Buffer (pH- 6.5) [61]. The observations were carried on under 10X magnification on Fluorescence Microscope at 460-610nm.

3.4.7 Transmission Electron Microscopy (TEM)

The TEM imaging was done by dropping 3 μL of amyloids formed with and without the influence of Proline and Pro-AuNP, on carbon coated TEM copper grids, followed by, dropping of 3 μL of 2% Phosphotungstic acid (PTA) [62]. The grids were then dried by desiccation and viewed under 200nm scale with high magnification under TEM. For the characterizsation of Cyt C amyloids Energy Dispersive X-ray Spectroscopic (EDS) analysis was done to spot the iron particles which disintegrate from the core of Cyt C when it fibrillates otherwise which remains intact in the core of the protein.

3.5 Docking Analysis

The PDB files of both HEWL (PDB ID: 3WUN) and Cyt C (2B4Z) were obtained from RCSB Protein Data bank (http://www.rcsb.org/pdb/home/home.do). The amino acid sequences of the proteins were obtained in FASTA format from the same and were fed into FoldAmyloid webserver which predicts the regions prone to amyloidosis by considering the physicochemical properties of the amino acids [63].

The structure of L-proline was obtained from PUBCHEM database in .sdf format and then converted to .pdb format using ONLINE SMILES TRANSLATOR. To identify the binding site of Proline, docking was done with HEWL and Cyt C in Patchdock server [64]. The binding energy analysis was done in Firedock [65].

The type of interaction between the protein and the ligand, and identification of the residues to which it binds, was analyzed by LIGPLOT, wherein, 2-D schematic representation of the Protein-ligand complex is automatically generated [66].

Chapter 4

Results and Discussion

4.1 Characterization of Proline Capped Gold Nanoparticles (Pro-AuNPs).

4.1.1 Ultraviolet- Visible (UV) Spectroscopy

The optical properties of Gold Nanoparticles (AuNps) are highly dependent upon their shape, size and surface functionality. It exhibits an optical characteristic called the Localized Plasmon Surface Resonance (LPSR), which can be defined as the collective oscillation of all the electrons occupying the conduction band of AuNPs which are in resonance to a particular wavelength of incident light. A single absorption peak is displayed by AuNPs at the range 500-600nm. In our study, the absorption spectra of Pro- AuNPs was measured in a Double Beam Spectrophotometer in the visible range 400 – 700nm and it showed heavy absorption at 529nm . For comparison, the same was measured for bare AuNPs (bAuNPs) was done. The bAuNPs showed absorption at 523nm. A red-shift in the absorption of bAuNPs to Pro-AuNPs was observed (Figure 4.1). The absorbance of Pro-AuNPs and bAuNPs were 1.070 and 1.186 respectively.

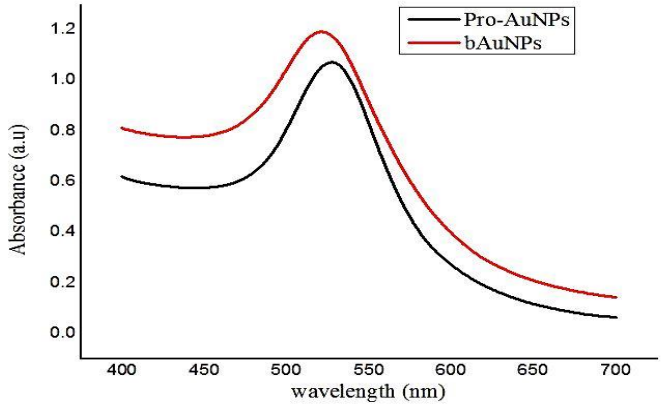

Figure 4.1: Absorbance spectra of Proline Capped Gold Nanoparticles (Pro-AuNPs) and bare Gold nanoparticles (bAuNPs) showing a slight red shift of peak for Pro-AuNPS indicating an change in optical properties and increase in diameter.

4.1.2 Particle Size distribution study by Dynamic Light Scattering (DLS)

The DLS analysis gives an approximate idea of particle size and particle size distribution. More specifically, it measures the hydrodynamic radius which is described as a sphere's size which would have the same translational diffusion co-efficient to that of a particle. In our study, we have used DLS as a technique to understand the size distribution of Pro-AuNPs And bAUNPs, and to check whether or not there was an increase in particle size of Pro-AUNPS from bAuNPs which would be an evidence of conjugation of proline to AuNPs. We have observed (Figure 4.2 & Figure 4.3) that the Z Average (d.nm) of bAuNP and Pro-AuNPs were 38.66 and 63.99 respectively. This shows that the particle size of AuNPs increased when proline conjugated with it. The Polydispersity index (PDI) value of bAuNps and Pro-AuNPs was 0.322 and 0.479. PDI value less than 0.7 signifies that there doesn't exist a broad size distribution. Also there were very small particles found which are shown in Table 4.1 & Table 42 for bAuNPs and Pro-AuNPs respectively.

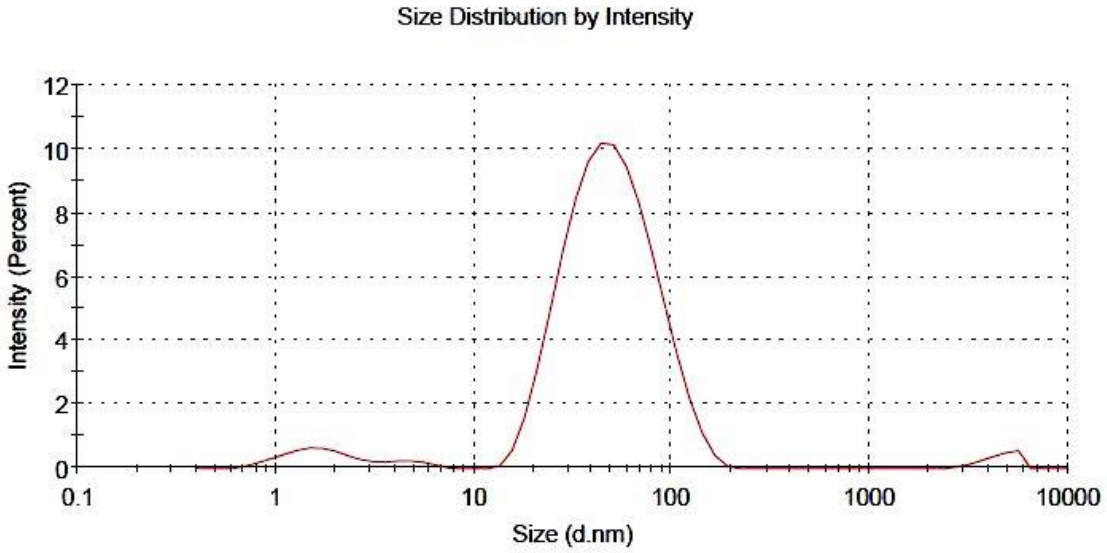

Figure 4.2: Size Distribution Graph of bAuNPs with Z Average (d.nm) 38.66 and PDI 0.322.

Table 4.1: List of size distribution Results obtained from DLS for bAuNPs.

	Size(d.nm)	% Intensity	St Dev(d.nm)
Peak 1	54.36	92.6	27.71
Peak 2	1.769	4.6	0.7190
Peak 3	4569	1.8	845.8

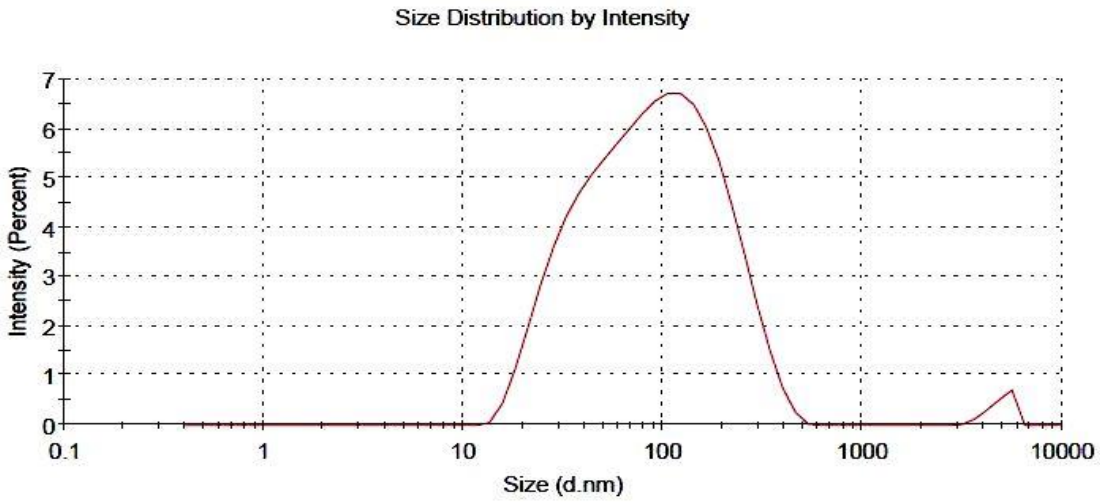

Figure 4.3 : Size distribution graph of Pro-AuNPs with z.average (d.nm) 63.99 and PDI 0.479

Table 4.2: List of size distribution Results obtained from DLS for Pro-AuNPs

	Size(d.nm)	% Intensity	St Dev(d.nm)
Peak 1	111.0	98.3	81.53
Peak 2	4896	1.7	674.6
Peak 3	0.000	0.0	0.000

4.1.9 Zeta Potential Distribution study

Zeta potential, which is the charge at the double layer, was measured in order to understand the electrostatic stabilization of bAuNPs and Pro-AuNPs. From the data obtained it is observed that the Zeta potential of bAuNPs and Pro-AuNPs were -22.7 and -29.3 (shown in Figure 4.4 & Figure 45 respectively). The increase in Zeta potential in the Pro-AuNPs is suggestive of the fact that Proline conjugation increased the stability of AuNPs. Moreover, the negative sign denotes a negative charge to the synthesized Pro-AuNPs.

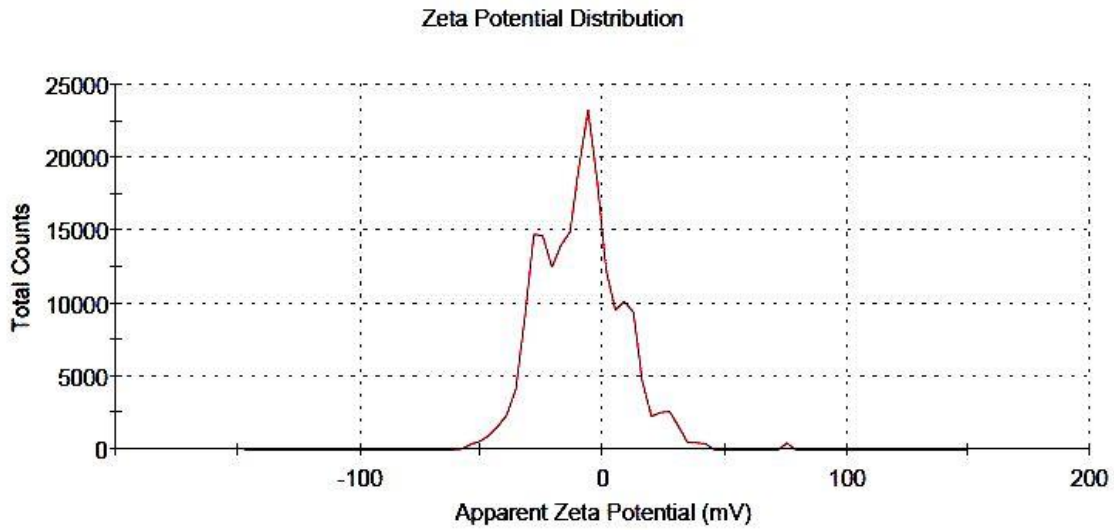

Figure 4.4: Zeta Potential of bAuNP (-22.7)

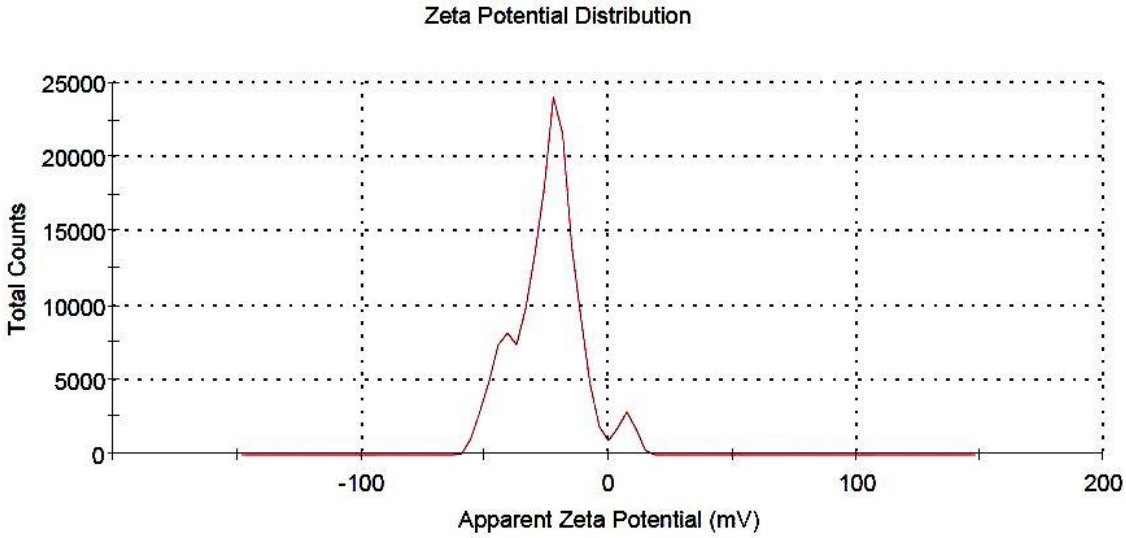

Figure 4.5. : Zeta Potential of Pro-AuNPs (-29.3)

4.1.10 Fourier Transform Infra-Red (FTIR) Spectroscopic analysis

The surface chemistry of the conjugation of Proline to that of the AuNP Surface was understood by FTIR analysis of Pro-AuNPs, bAuNps and bare Proline (shown in Figure 4.6) The typical peaks of bare proline are also observed in the Pro-AuNPs with a shift of peak which is an indication of conjugation. The Peak at 1601.26 cm^{-1} for Amide N-H Bending in the bAuNP shifted to 1588.1 cm^{-1}. The –C-H Bending peak 1413.33 cm^{-1} of bAuNP shifted to 1307.85 cm^{-1} in Pro-AuNP. Similar peak shift was observed for C-N Stretch (1335.99 cm^{-1} to 1322.8 cm^{-1}), C-H Stretch (3030.42cm^{-1} to 3023.46cm^{-1}) and Amide N-H Stretch

(3741.90cm^{-1} to 3728.75 cm^{-1}). It is anticipated that the conjugation has taken place by the amide- group of the Proline onto the surface of the Gold nanoparticles. The surface chemistry suggested that the proline interacted with Gold by N-Au interaction as studies by Rai et al [51] There are two ways of interaction: firstly, because proline was at a pH lower than its pI, it had attained positive charge whereas the AuNPs synthesized by Turkevich method were negatively charged. The unreduced gold ions which remained in the solution were also reduced by proline as reported by Mu et al in 2013 [67]. Possibility is that Au^{3+} ions were reduced by the lone pair electron of nitrogen of the pyrrolidone ring of proline.The FTIR analysis of bAUNP also showed no significant peaks owing to their lack of functional groups. A weak citrate adsorption on the surface of the bAuNP for which it attains a negative might have been removed during the centrifugation process during the sample preparation of FTIR. Therefore, no significant peaks are exhibited by bAuNPs.

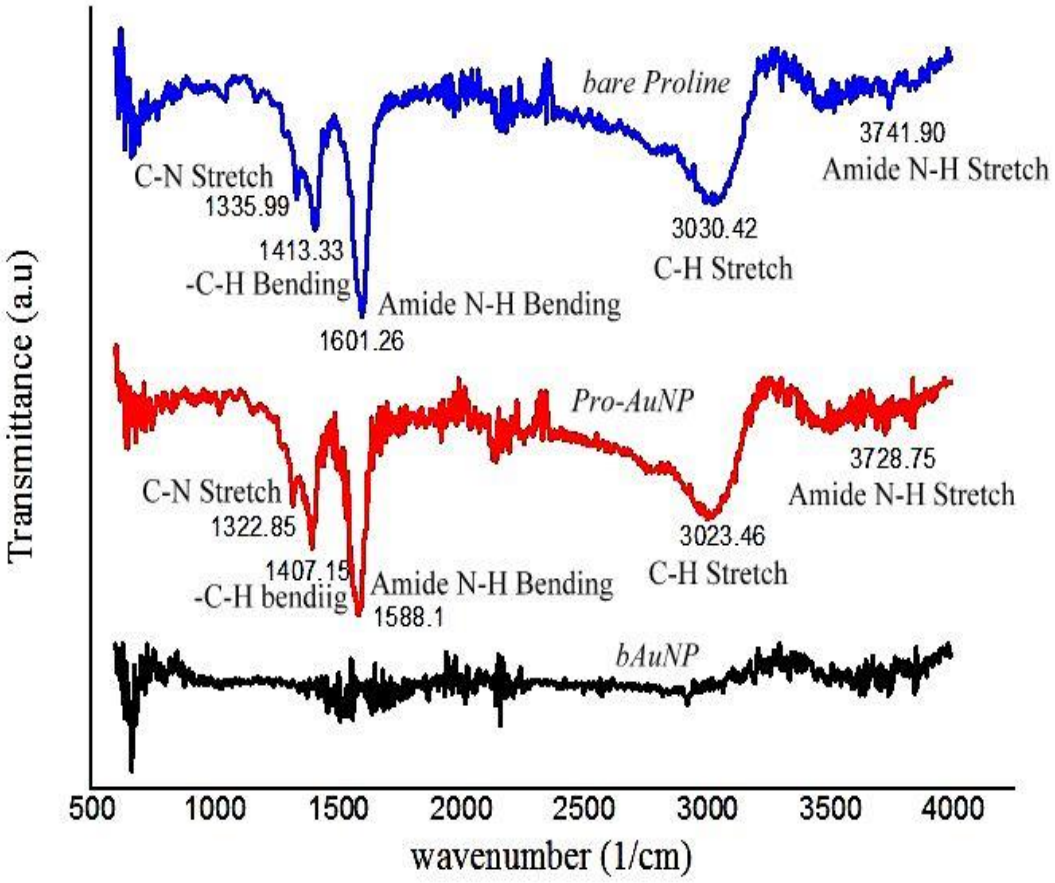

Figure 4.6: FTIR spectra of bare Proline, Pro-AuNPs and bAuNPs showing typical peaks of proline to be present in Pro-AuNPs and no significant peak for bAuNPs.

4.1.5 Transmission Electron Microscopy (TEM)

The morphological analysis of the Pro-AuNPs and its comparison with bAuNPs was done using TEM imaging (Figure 4.7). Another set of images (Figure 4.8) were collected after two months of synthesis in order to validate the results of Zeta potential, i.e, check whether the Pro-AuNPs are more stable than the bAuNPs which is also an indication of conjugation as the surface functionality with proline is stronger than Citrate adsorption. The TEM images show that the Size and shape of the Pro-AuNPs and bAuNPs is similar with slight increase in diameter in case of Pro-AuNPs which is due to the conjugation of Proline. Average diameter of the bAuNPs was found to be 25 ± 5nm and Pro-AuNPs was 30± 5 (Figure 4.9). The lattice fringes of the bAuNPs and Pro-AuNPs reveal they are of crystalline nature (Figure 4.10) and spacing was found to be 0.21nm and 0.23nm for a bAuNP (Figure 4.11) and a Pro-AuNP (Figure 4.12) respectively. The similarity of the bAuNPs to the Pro-AuNPs makes it a perfect candidate for control experiment to screen the effect of AuNPs on HEWL and Cyt C.

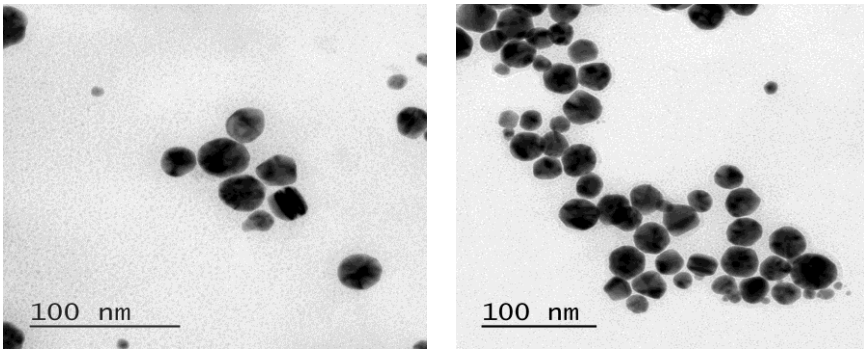

(a) (b)

Figure 4.7 (a): High Resolution TEM image of Pro-AuNPs (taken after two weeks of synthesis) (b): High Resolution TEM image of bAuNPs (taken after two weeks of synthesis)

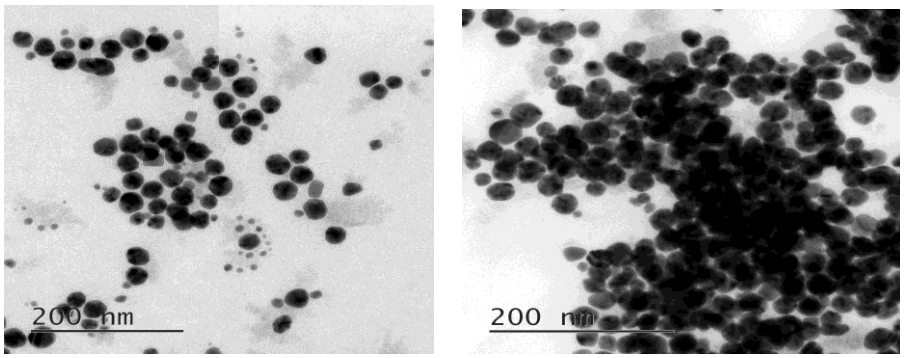

(a) (b)

Figure 4.8 (a) High Resolution TEM image of Pro-AuNPs (taken after two months of synthesis) (b)High Resolution TEM image of bAuNPs (taken after two months of synthesis)

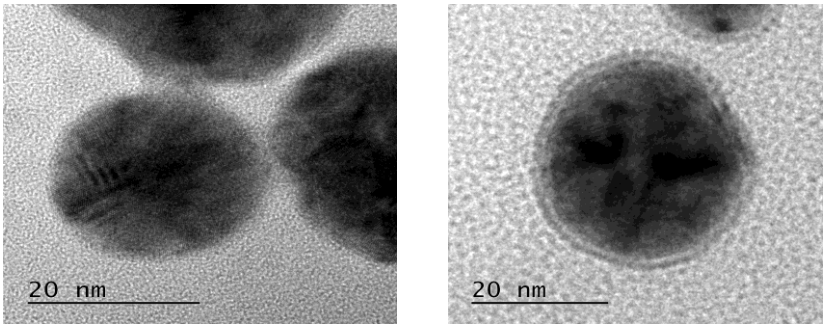

(a) (b)

Figure 4.9 (a) Size of a bAuNP (25nm approx) (b): Size of a Pro-AuNP (38 approx)

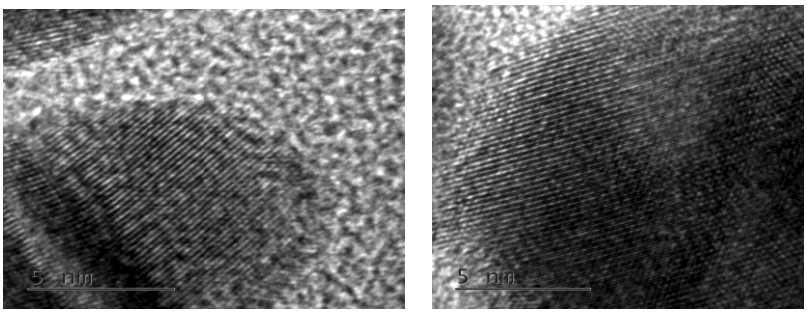

(a) (b)

Figure 4.10 (a) Lattice fringes of bAuNPs (b) Lattice fringes of Pro-AuNPs. showing that they are of crystalline nature.

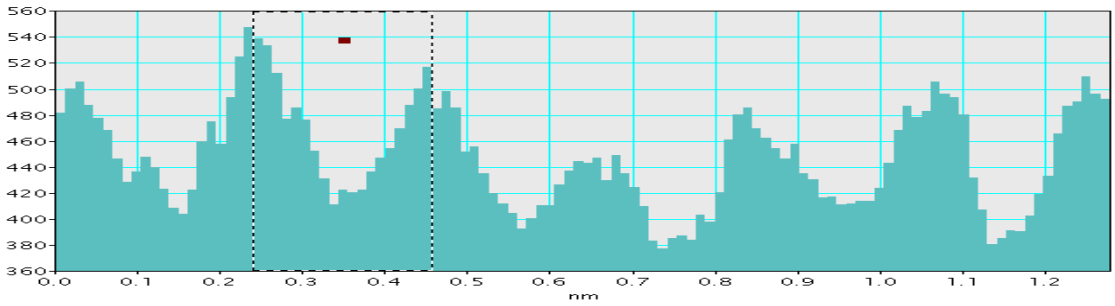

Figure 4.11 Spacing profile of lattice fringes of bAuNPs showing a 0.21nm spacing

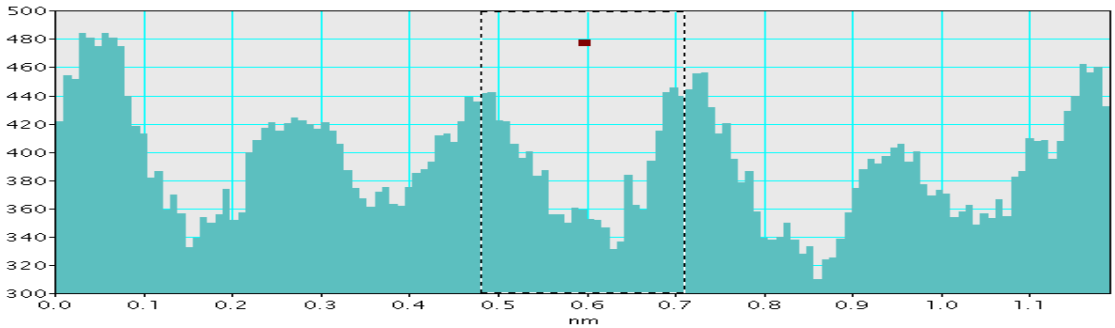

Figure 4.12 Spacing profile of lattice fringes of Pro-AuNPs showing a 0.23nm spacing

4.1.6 X-Ray Energy Dispersive Spectrometry (EDS)

The elemental analysis of the bAuNPs and Pro-AuNPs was done in the mode X-Ray Energy Dispersive Spectroscopy (EDS) of TEM. The composition and the quantification of the elements present in the AuNPs can be analyzed using EDS. In our study, the EDS graph shows that Pro-AuNPs has Nitrogen (Figure 4.14) which is possibly from the secondary amine group of proline- yet another indication that proline was absorbed on the surface of the AuNPs. on the contrary the bAuNPs do not have the nitrogen peaks (Figure 4.13).

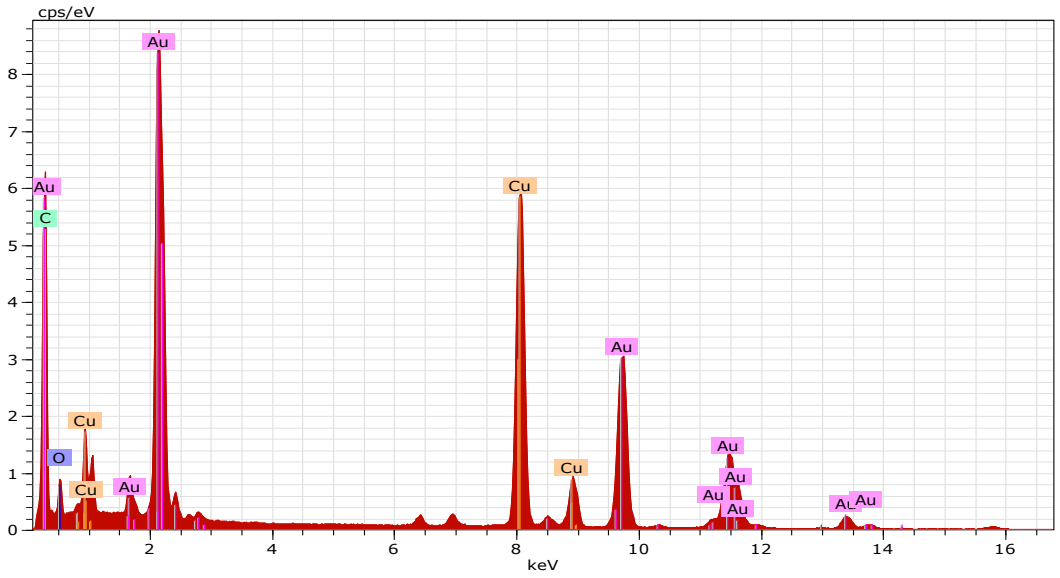

Figure 4.13: EDS Spectrum of bAuNPs

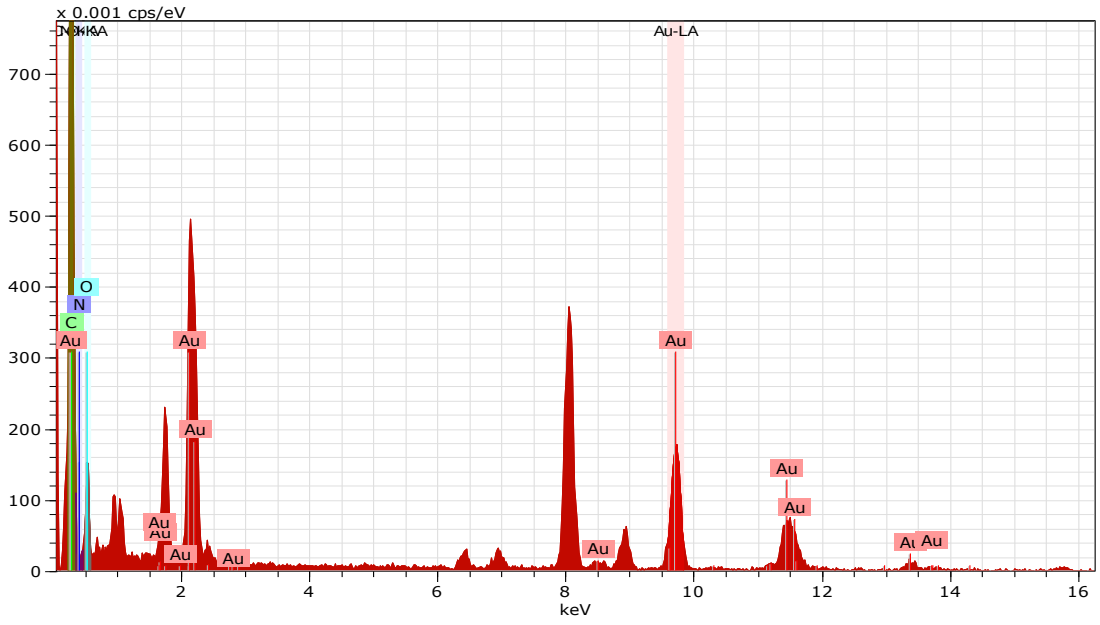

Figure 4.14: EDS Spectrum of Po-AuNPs

4.1.7 Scanning Transmission Electron Microscopy (STEM)

The elemental mapping was done in STEM, wherein, a High Angle Annular Dark Field (HAADF) detector detects transmitted electron scattered though a relatively large angle. in our study, the mapping of Gold (Au), Carbon (C), oxygen(O) and nitrogen (N) of Pro-AuNPs was done and is shown in Figure 4.15.

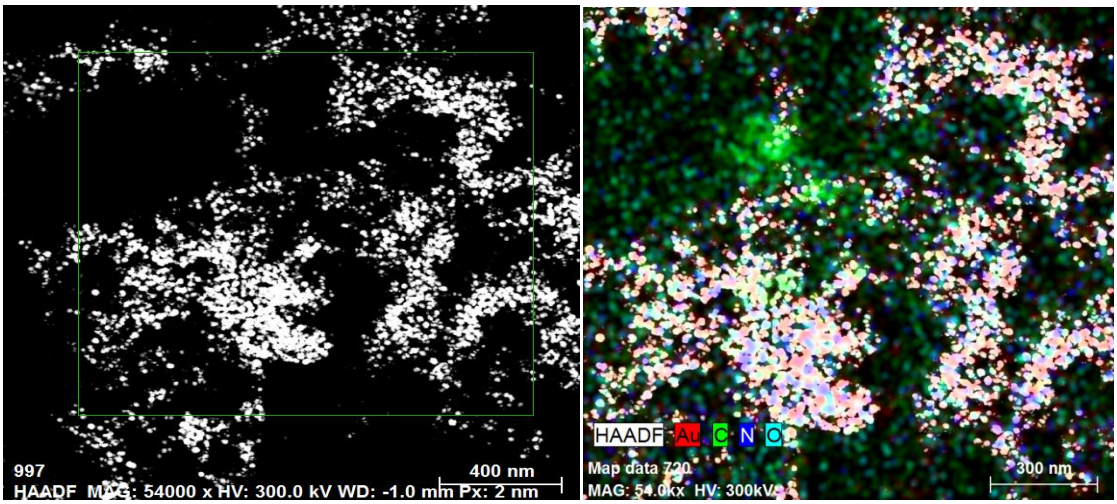

(a) (b)

Figure 4.15 (a): Dark field image of Pro-AuNPs with the marked region used for STEM. (b): STEM image of of Pro-AuNPs

4.1.8 Selected Area Diffraction (SAED)

Selected Area Diffraction (SAED) is a technique wherein a parallel beam of high energy electrons are treated as wave like and the crystalline specimen is subjected to it. Atoms in the specimen act as diffraction grating to the electrons, which are thereby diffracted. Polycrystalline substances give a ring pattern. In our study, we have attempted to understand the crystalline nature of the Pro-AuNPs by SAED. The Selected Area Diffraction pattern (SADP) (Shown in Figure 4.16) exhibits ring formation which is an indication that the Pro-AuNPs are slightly polycrystalline. This is due to the fact, that during the process of conjugation by aging proline with bAuNPs, some of the proline molecules also reduce the unreduced Gold ions present in the solution. Pro-AuNPs were found to have a larger size distribution in DLS study which can be attributed to the fact that there are two types of Pro-AuNPs synthesized- Predominantly reduced by Trisodium citrate and proline capped by aging, the other type being, although in lesser magnitude, the gold ions reduced by Proline itself.

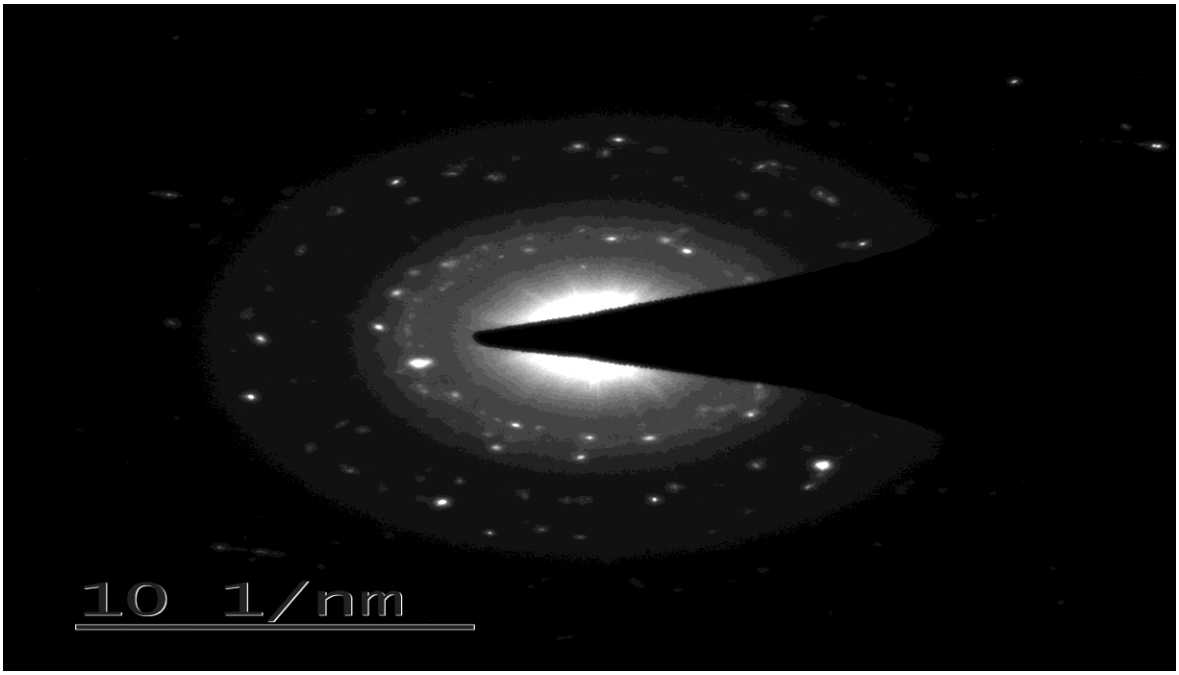

Figure 4.16: SADP of Pro-AuNPs showing ring formations typical of polycrystalline substances.

4.2 Synthesis and characterization of Hen Egg White Lysozyme (HEWL) and Cytochrome C (Cyt C)

The amyloids of HEWL were synthesized at 55 °C in 10mM Glycine-HCl buffer maintained at pH-2 and Cytochrome C amyloids were synthesized at 75°C in 10mM Tris-HCl buffer maintained at pH 9. The TEM images (Figure 4.17) of the respective amyloids revealed their distinct morphology. The HEWL Amyloids were found to be 12 to 15 nm in diameter forming a mesh, although themselves individually long. Whereas the Cyt C amyloids are long, straight, with 50 to 55 nm in diameter, and relatively scattered. There were small particle of range within 10nm which were seen alongside the Cyt C amyloids and the EDS spectra revealed that they were formed of iron. Iron is found to be present in the heme group of Cyt C which keeps the native structure intact, and Cyt C amyloidogenesis happens alongside the loss of heme group. Therefore, the presence of iron in free state proves that Cyt C fibrillation ejects out iron from its native structure.

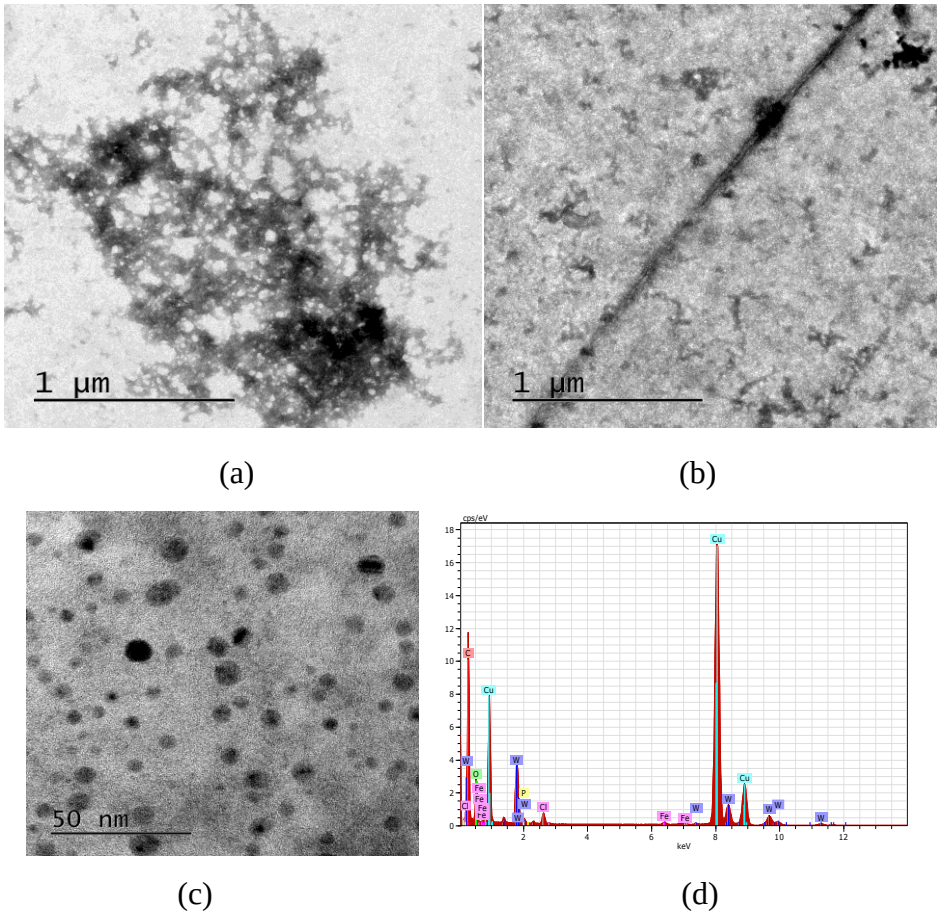

Figure 4.17 (a) Hen Egg white Lysozyme (HEWL) amyloid imaged at 1 µm scale showing a meshed formation (b) Long straight amyloid of Cytochrome C taken at 1 µm scale (c) Small particles within 10nm observed alongside Cyt C amyloids imaged at 50nm (d) : EDS elemental analysis showing the presence of iron in the small particles.

4.3Inhibition Profiles

4.3.1 Thioflavin T Assay

Thioflavin T is a dye that binds with amyloid fibrils and gives an amplified flurorescence. ThT was used in our study to monitor the inhibition of Proline and Pro- AuNPs towards the fibrillation of HEWL and Cyt C. HEWL and Cyt C were incubated in the amyloidogenic condition in the presence of the same (Proline- 1:20 molar ratio and Pro-AuNPs- 100µL) and also bAuNP (100µL) to screen any inhibitory effect by the bAuNPs themselves. Our results show that the flurescence curve was sigmoidal which is characteristic of amyloid. HEWL and Cyt C samples incubated without Proline and Pro-AuNPs showed significant increase in flurescence than the sample in their presence. Inhibition of Pro-AuNPs is higher than bare

Proline whereas bAuNPs (as synthesized in our study) were found to be ineffective in inhibiting amyloid formation. Also the pattern of HEWL and Cyt C was similar.

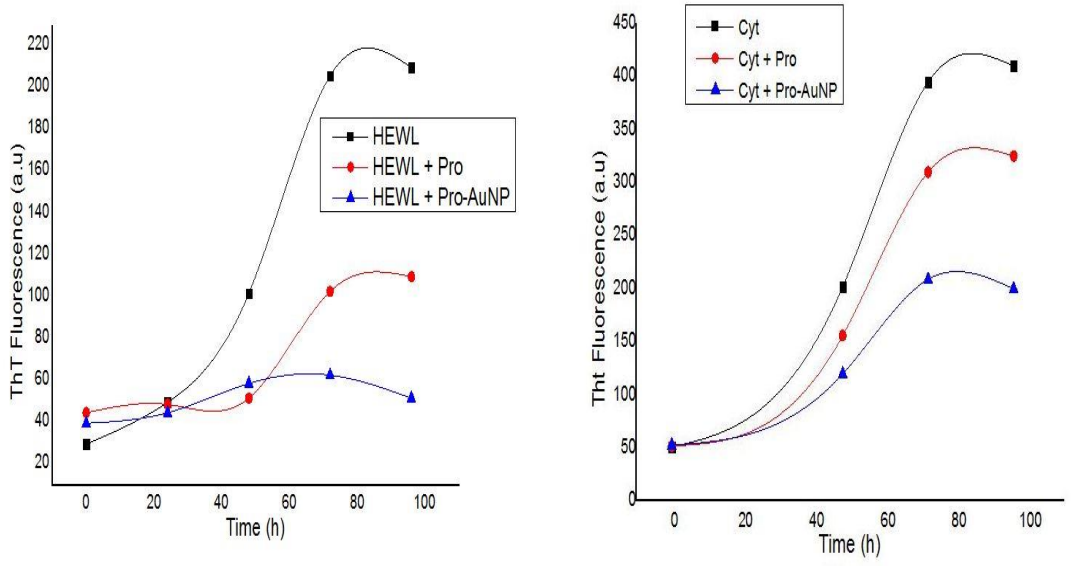

(a) (b)

Figure 4.18 (a) Thioflavin T inhibition profile of Proline (Pro) and Proline capped Gold nanoparticles (Pro-AuNPs) on Hen Egg White Lysozyme (HEWL) (b) Thioflavin T inhibition profile of Proline (Pro) and Proline capped Gold nanoparticles (Pro-AuNPs) on Cytochrome C (Cyt C)

4.3.2 1- Anilinonaphthalene- 8- sulphonic (ANS) Acid Binding Assay

ANS is a dye which binds to the hydrophobic patches of proteins when they are exposed in the process of unfolding and gives enhanced fluorescence. In amyloidogenesis too, hydrophobic residues are exposed which are otherwise present at the core of the protein. In our study, we have used ANS assay to understand the conformation changes occurring during amyloid formation in HEWL and Cyt C which are unrelated structurally. It is observed that, when HEWL and Cyt C are incubated with Proline and Pro-AuNP, it gives lesser flurescence than the one without. The pattern of the inhibition is also similar in both HEWL and Cyt C (Figure 4.19).

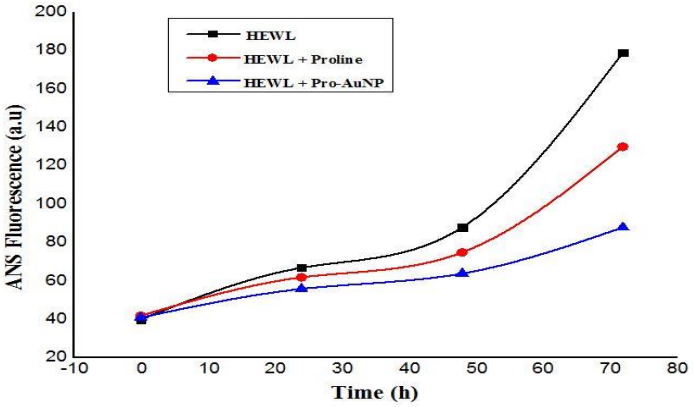

(a)

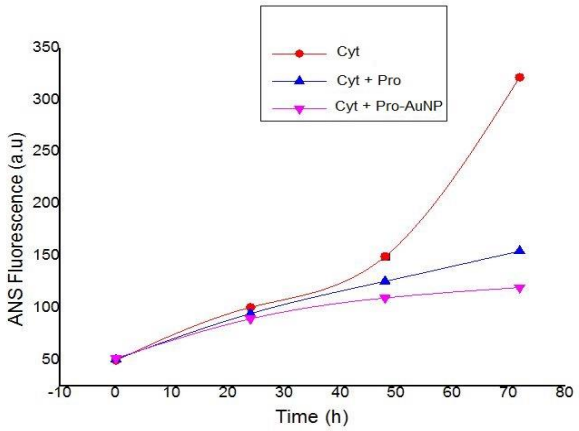

(b)

Figure 4.19 (a) 1-Anilinonaphthalene-8-sulfonate (ANS)fluorescence vs. time curve for HEWL, HEWL incubated with Proline (Pro) and Pro-AuNPs (b) 1-Anilinonaphthalene-8-sulfonate (ANS)fluorescence vs. time curve for Cyt C, Cyt C incubated with Proline (Pro) and Pro-AuNPs.

The pattern suggests that as the proteins unfold the way hydrophobic residues are exposed are similar in both the proteins, which is why, the binding of ANS to the residues is also similar. Although, the two proteins are very different in structure and in their content of hydrophobic residues, the similar pattern is indicative of a common pathway of amyloidogenesis with exposed hydrophobic patches in common intermediate structures. Proline and mror profoundly Pro-AuNPs, bind to intitial intermediates and arrest them in “aggregation insensitive” states as described Samuel et al, 2000 [44].

4.3.3 Tryptophan Intrinsic Flurescence

Intrinsic fluorescence is the fluorescence emitted by tryptophan residues alone excited at 295nm. Tryptophan is a hydrophobic aromatic amino acid which in the unfolded states of a protein gets exposed and fluoresces. In our study, intrinsic fluorescence was performed after 72 hours of incubation of HEWL and Cyt C with and without the presence of Proline and Pro-AuNPs. It is observed (Figure 4.20) that after 72 hours, there was significant amount of tryptophan fluorescence in the HEWL and Cyt C incubated without the presence of Proline and Pro-AuNPs, whereas, a pronounced decrease was seen in HEWL with the presence of the same and, although not as significant as HEWL, Cyt C incubated with the aforementioned also showed a similar pattern of intrinsic flurorescence profile.

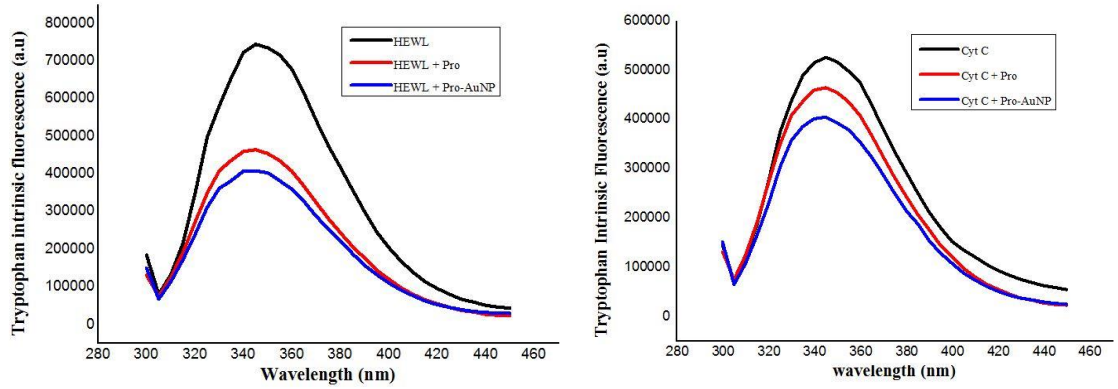

(a) (b)

Figure 4.20 (a) Tryptophan intrinsic Fluorescence assay: Fluorescence (a.u) Vs wavelength (nm) Curve for HEWL, HEWL incubated with Proline (Pro) and Pro-AuNPs. (b) Tryptophan intrinsic assay: Fluorescence (a.u) Vs wavelength (nm) Curve for Cyt C, Cyt C incubated with Proline (Pro) and Pro-AuNPs.

4.3.4 Fluorescence Microsocopy

Figure 4.21 shows Fluorescence microscopy images obtained at the 0^{th} hour prior to the incubation of HEWL showed almost nil fluorescence but after 72 hours of incubation showed significant increase in fluorescence indicating that dense amyloid formation has taken place. In samples incubated with Proline, there is significant decrease in fluorescence and with Pro-AuNPs there is almost nil fluorescence like that of the monomeric HEWL.

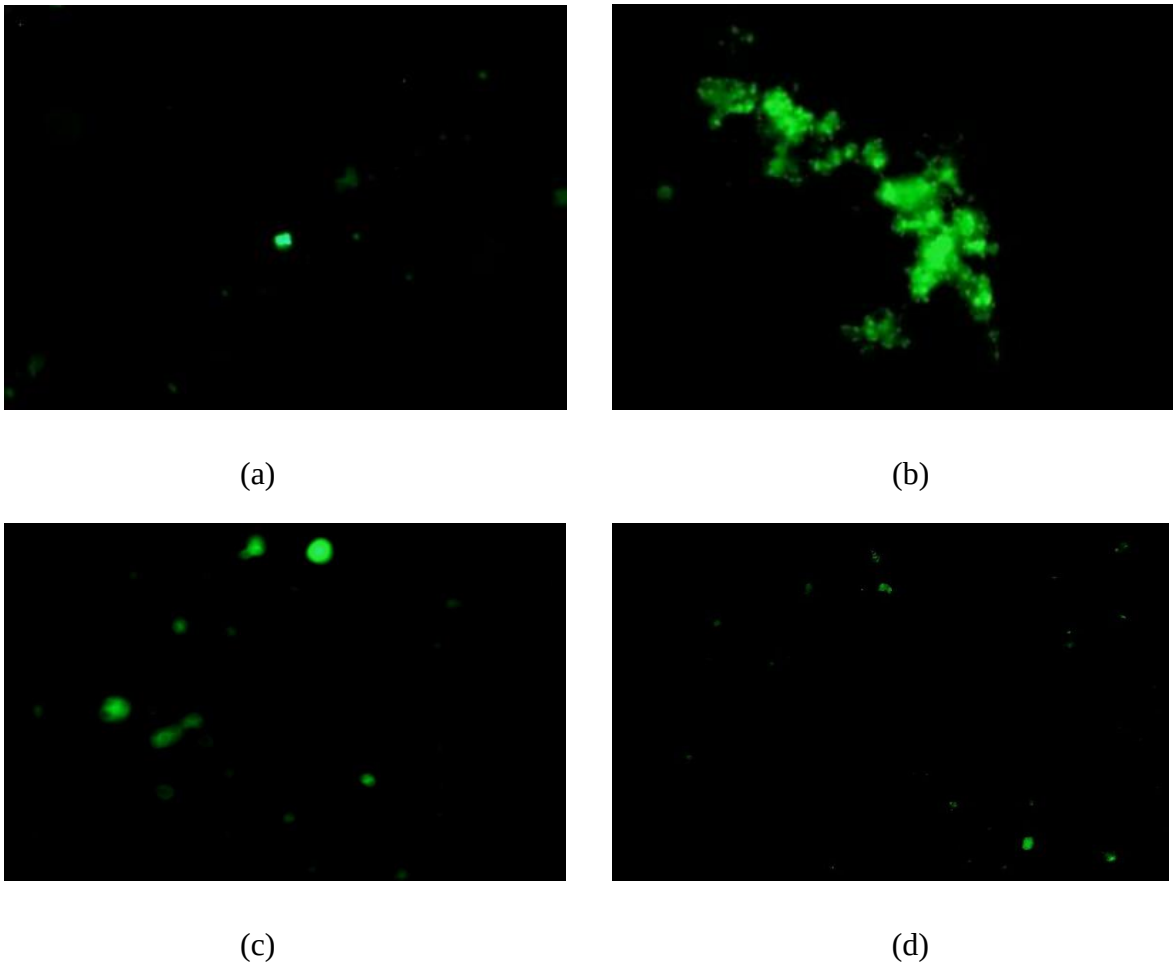

(a) (b)

(c) (d)

Figure 4.21. (a) Fluorescence Microscopy image of monomeric HEWL showing almost nil fluorescence taken at 0^{th} hour. (b) Fluorescence Microscopy image of HEWL amyloid showing significant fluorescence taken at 72^{th} hour. (c) Fluorescence Microscopy image of HEWL incubated with proline showing significant reduction of fluorescence taken at 72^{th} hour. (d) Fluorescence Microscopy image of HEWL incubated with Pro-AuNPs showing almost nil of fluorescence taken at 72^{th} hour.

4.3.5 Transmission Electron Microscopy (TEM)

Figure 4.22 shows the TEM images of HEWL and Cyt C amyloids alongside the samples incubated with Proline and Pro-AuNPs. it is observed that HEWL mature fibrils are formed with distinct morphology and are densly meshed. The presence of Proline somewhat arrests the HEWL in an intermediate misfolded state whereas we see a complete inhibition of amyloidogenesis with the presence of Pro-AuNPs. A disaggregation experiment was also caaried out with Pro-AuNPs and it was found that the mature fibrils were disintegrated when incubated with Pro-AuNPs Similar results are found with Cyt C (Figure 4.23) wherein, yet

again Proline partially inhibits Cyt C amyloid formation. Pro-AuNPs inhibits the process of amyloids almost completely.

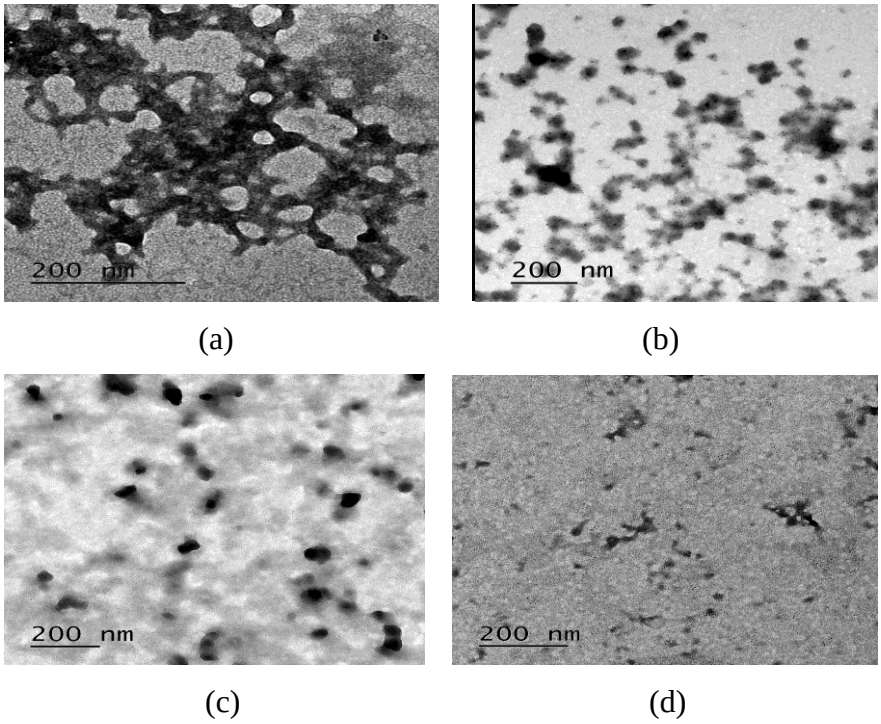

(a) (b)

(c) (d)

Figure 4.22. (a) Mature amyloid fibrils of HEWL alone showing stable and dense fibrillar formations (b) HEWL incubated with Proline alone showing intermediate structures between oligomeric state and fibrils. (c) Complete inhibition of HEWL amyloid fibrillation by Pro-AuNPs showing distinct oligomeric states. (d) Disaggregation study performed on HEWL mature amyloids by incubating with Pro-AuNPs for 36 hours at 37°C showing disintegrated fibrils

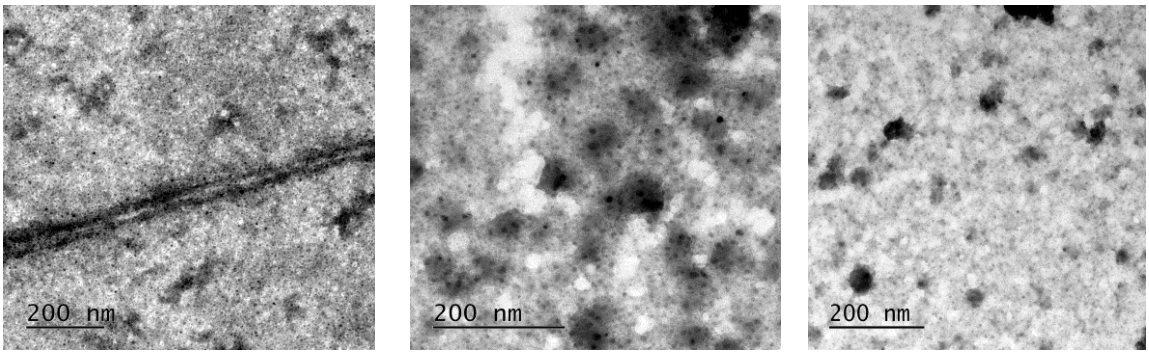

(a) (b) (c)

Figure 4.23 (a) Mature amyloid of Cyt C showing distinct straight morphology (b) Cyt C incubated with Proline showing intermediate structures about to fibrillate after oligomeric state (c) Cyt C incubated with Pro-AuNPs showing distinct oligomeric states of Cyt C.

4.4 Computational methods: prediction of amyloidogenic region, binding site of Proline to HEWL and Cyt C & interaction analysis

Amyloidogenic region of the proteins HEWL and Cyt C were predicted using FoldAmyloid online server. In HEWL, the residues from 26-30, 60-64, 106-113 and 121-129 play role in the amyloidogenesis of the same. The docking of Proline with HEWL using patchdock web server gave a binding energy of -15.19 Kcal/mol. The residues with which it interacts are Ala107 (nearby amyloidogenic region), Trp108 (in amyloidogenic rgion), Asp52, Gln57 and Asn59 (both nearby amyloidogenic region). The interaction is predominantly hydrophobic and a 2.48Å long hydrogen bond formation takes place between the nitrogen (of Pyrrollidone Ring) and carbonyl oxygen of Gln57 of HEWL.

In Cyt C, two regions were found to be amyloidogenic- residues 33-37 and 80-84. The docking of Proline with Cyt C gave a binding energy output -9.48 Kcal/mol. The residues with which Proline interacted are Ile81, Phe82, Ala83 (All in amyloidogenic region) and Lys72. The interactions are solely hydrophobic. The results indicate that not only hydrophobicity plays an important role in amyloidogenesis but also plays an important role in its inhibition.

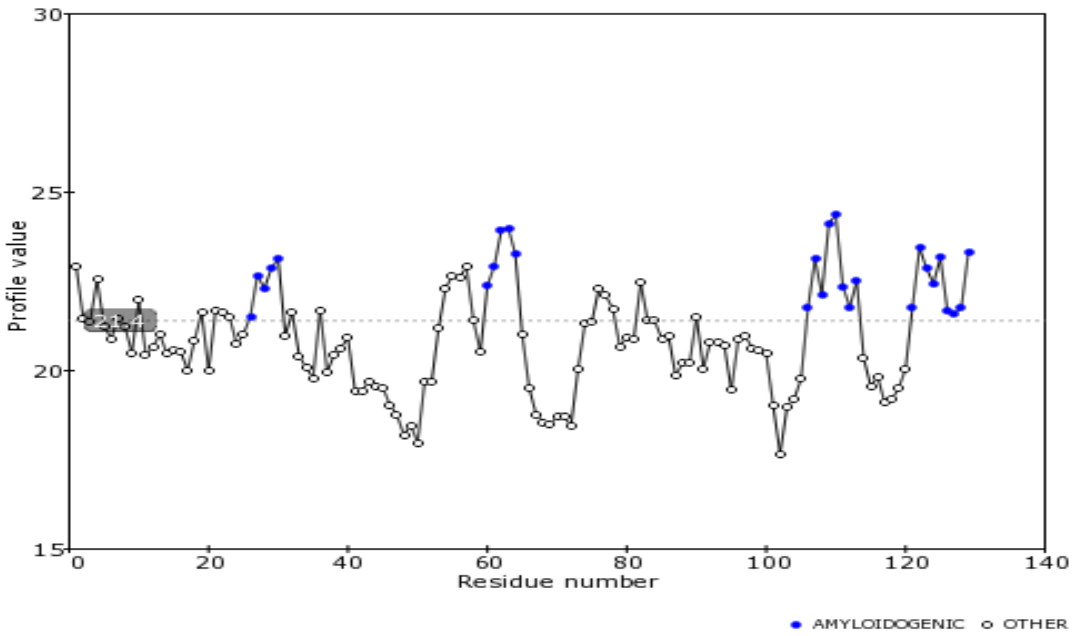

Figure 4.24 (a) FoldAmyloid prediction of amyloidogenic regions of HEWL

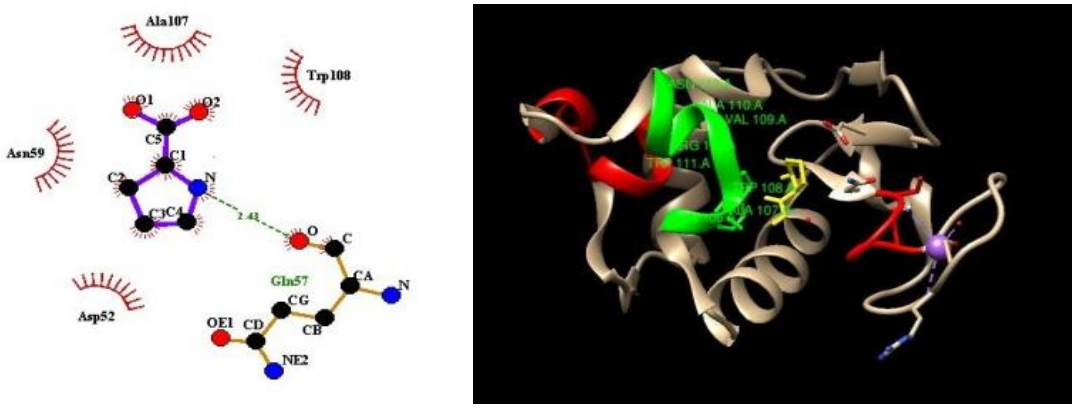

(b) (c)

Figure 4.24. (b) LIGPLOT Analysis of docked complex of proline with HEWL(c) Chimera view of the docked complex of proline with HEWL showing the amyloidogenic regions and the interacting residues.

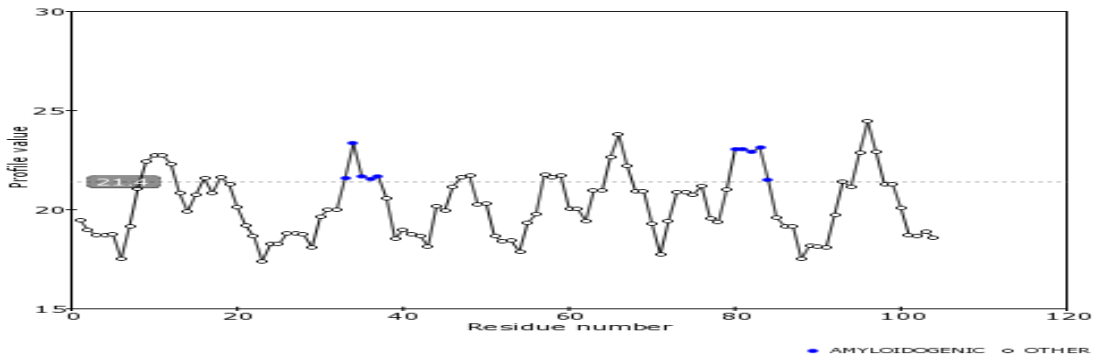

(a)

(b) (c)

Figure 4.25 (a) FoldAmyloid prediction of amyloidogenic regions of Cyt C. (b) LIGPLOT Analysis of docked complex of proline with HEWL. (c) Chimera view of the docked complex of proline with Cytochrome C showing the amyloidogenic regions and the interacting residues.

Chapter 5

Conclusion

Proline capped Gold nanoparticle (Pro-AuNPs) were synthesized and vigorously characterized by a combination of established methods. It was followed by testing their potentiality to inhibit the amyloidogenesis of two completely unrelated proteins- HEWL and Cyt C. For comparison on the effect of gold nanoparticle functionalization, bare proline was also separately used for the inhibition study. Various methods like ThT assay, ANS assay, Intrinsic fluorescence assay, CD spectroscopy, Fluorescence microscopy, TEM and computational docking studies were performed to monitor, visualize and understand the mechanism of amyloidogenesis for both the proteins. Our results reveal that both the proteins show a similar pattern of inhibition. Proline is a well known chemical chaperone (Choudhary et al 2016) and the capping of Gold nanoparticles with amino acids also increases their anti-amyloidogenic propensity Proline was found to inhibit the amyloidogenesis of HEWL and Cyt C in a similar pattern. The inhibition pronounced when proline was capped to AuNPs. The possible reason is the increase of local concentration of proline when capped to AuNPs. Also the polycrystalline nature of the Pro-AuNP also increases the surface area of action as certain conformations could also reached by the presence of very small Pro-AuNPs which can penetrate, like we have seen in the disaggregation of HEWL with Pro-AuNPs, wherein, Pro-AuNPs could penetrate the beta sheets of amyloids and break them (Li 1996). The ANS results reveal a common exposure of hydrophobic residues for both HEWL and Cyt C which in the presence of proline and Pro-AuNPs was inhibited. Possible reason is that proline, bare or attached, is hydrophobic by nature, so, when hydrophobic patches of the proteins were exposed initially, they interacted with the exposed hydrophobic residues with hydrophobic interaction and arrested the structure in an “aggregation insensitive” state. The intrinsic fluorescence also shows a similar pattern of inhibition for both HEWL and Cyt C. TEM images of both the proteins reveal that the proline and more profoundly Pro-AuNPs arrest the amyloidogenesis at the oligomeric state, preventing the formation of the critical nucleus essential for further fibrillation. The docking study of Proline suggested rich hydrophobic interaction with the amyloidogenic residues and also the neighbouring residues. For Cyt C, the interactions were purely hydrophobic and in case of HEWL, a hydrogen bond formation was formed between the nitrogen (of Pyrrollidone Ring) and carbonyl oxygen of Gln57 of HEWL. Another aspect our research focused was the effect of charge. HEWL (pI 11.35) and

Cyt C (pI 10) were incubated at pH 2 and pH 9 wherein both the proteins attain positive charge in various degrees. Proline (pI 6.3) on the other hand attains positive charge at pH 2 and negative charge at pH9. But a common inhibition irrespective of the charge of the inhibitor and the protein suggests that the charge plays no or minor role in the inhibition of amyloidogenesis, rather the structure of the inhibitor is important. Our previous study with Polyvinyl pyrrolidone suggests that the pyrrolidone ring might exert an inhibiting effect as proline too is chemically structured upon pyrrolidone ring by Tulika et al 2017 [68]. Also, the isoelectric point (or pI) of the proteins seem to play no role, an inference also drawn by Shiraki et al, 2002.

We conclude with our current studies that amyloidogenesis follows a common route to culminate irrespective of the structure of the protein of origin. The charge of both, the inhibitor and the protein, plays no or minor role in the whole process. The structure of inhibitor rather plays the important role. We also conclude that not only hydrophobic interaction is the driving force of amyloidogenesis but it can also be exploited to inhibit the process. Due to the fact, that the pattern of amyloidogenesis is similar, it is also possible to develop a common inhibitor for all amyloidosis.

References

[1] Dobson, Christopher M. "Protein folding and misfolding." *Nature* 426, no. 6968 (2003): 884-890.

[2] Dill, Ken A., and Hue Sun Chan. "From Levinthal to pathways to funnels." *Nature structural biology* 4, no. 1 (1997): 10-19.

[3] Radford, Sheena E., and Christopher M. Dobson. "From computer simulations to human disease." *Cell* 97, no. 3 (1999): 291-298.

[4] Wolynes, Peter G., Jose N. Onuchic, and D. Thirumalai. "Navigating the folding routes." *SCIENCE-NEW YORK THEN WASHINGTON*- (1995): 1619-1619.

[5] Tsemekhman, Kiril, Lukasz Goldschmidt, David Eisenberg, and David Baker. "Cooperative hydrogen bonding in amyloid formation." *Protein science* 16, no. 4 (2007): 761-764.

[6] Sipe, Jean D., and Alan S. Cohen. "Review: history of the amyloid fibril." *Journal of structural biology* 130, no. 2-3 (2000): 88-98.

[7] Naito, Akira, et al. "Structural diversity of amyloid fibril formed in human calcitonin as revealed by site- directed 13C solid- state NMR spectroscopy."*Magnetic Resonance in Chemistry* 42.2 (2004): 247-257.

[8] Hartl, F. Ulrich, and Manajit Hayer-Hartl. "Molecular chaperones in the cytosol: from nascent chain to folded protein." *Science* 295, no. 5561 (2002): 1852-1858.

[9] Bukau, Bernd, and Arthur L. Horwich. "The Hsp70 and Hsp60 chaperone machines." *Cell* 92, no. 3 (1998): 351-366.

[10] Schubert, Ulrich, Luis C. Anton, James Gibbs, Christopher C. Norbury, Jonathan W. Yewdell, and Jack R. Bennink. "Rapid degradation of a large fraction of newly synthesized proteins by proteasomes." *Nature* 404, no. 6779 (2000): 770-774.

[11] Anfinsen, Christian B. "Studies on the principles that govern the folding of protein chains." (1972).

[12] Anfinsen, Christian B., Edgar Haber, Michael Sela, and F. H. White. "The kinetics of formation of native ribonuclease during oxidation of the reduced polypeptide chain." *Proceedings of the National Academy of Sciences* 47, no. 9 (1961): 1309-1314.

[13] Dill, Ken A., and Hue Sun Chan. "From Levinthal to pathways to funnels." *Nature structural biology* 4, no. 1 (1997): 10-19.

[14] Durup, Jean. "On “Levinthal paradox” and the theory of protein folding." *Journal of Molecular Structure: THEOCHEM* 424, no. 1-2 (1998): 157-169.

[15] Berezovsky, Igor N., and Edward N. Trifonov. "Loop fold structure of proteins: resolution of Levinthal's paradox." *Journal of Biomolecular Structure and Dynamics* 20, no. 1 (2002): 5-6.

[16] Kumar, Santosh, and Jayant B. Udgaonkar. "Mechanisms of amyloid fibril formation by proteins." *Curr Sci* 98.5 (2010): 639-56.

[17] Soto, C. (2001). Protein misfolding and disease; protein refolding and therapy. *FEBS letters*, *498*(2), 204-207.

[18] refercnce: Sgarbossa, A. (2012). Natural biomolecules and protein aggregation: emerging strategies against amyloidogenesis. *International journal of molecular sciences*, *13*(12), 17121-17137

[19] Makin, O. Sumner, Pawel Sikorski, and Louise C. Serpell. "Diffraction to study protein and peptide assemblies." *Current opinion in chemical biology*10.5 (2006): 417-422.

[20] Der-Sarkissian, Ani, et al. "Structural organization of α-synuclein fibrils studied by site-directed spin labeling." *Journal of Biological Chemistry*278.39 (2003): 37530-37535.

[21] Tycko, Robert. "Insights into the amyloid folding problem from solid-state NMR." *Biochemistry* 42.11 (2003): 3151-3159

[22] Goldsbury, Claire, et al. "Watching amyloid fibrils grow by time-lapse atomic force microscopy." *Journal of molecular biology* 285.1 (1999): 33-39.

[23] Naito, Akira, et al. "Structural diversity of amyloid fibril formed in human calcitonin as revealed by site- directed 13C solid- state NMR spectroscopy."*Magnetic Resonance in Chemistry* 42.2 (2004): 247-257

[24] Makin, O. Sumner, Pawel Sikorski, and Louise C. Serpell. "Diffraction to study protein and peptide assemblies." *Current opinion in chemical biology*10.5 (2006): 417-422.

[25] Vieira, Marcelo NN, J. Daniel Figueroa-Villar, M. Nazareth L. Meirelles, Sérgio T. Ferreira, and Fernanda G. De Felice. "Small molecule inhibitors of lysozyme amyloid aggregation." *Cell biochemistry and biophysics* 44, no. 3 (2006): 549-553.

[26] Momany, F. A., R. F_ McGuire, A. W. Burgess, and Harold A. Scheraga. "Energy parameters in polypeptides. VII. Geometric parameters, partial atomic charges, nonbonded interactions, hydrogen bond interactions, and intrinsic torsional potentials

for the naturally occurring amino acids." *The Journal of Physical Chemistry* 79, no. 22 (1975): 2361-2381.

[27] Reddy, K., Ravi Charan, Hauke Lilie, Rainer Rudolph, and Christian Lange. "l- Arginine increases the solubility of unfolded species of hen egg white lysozyme." *Protein Science* 14, no. 4 (2005): 929-935.

[28] Xiao, Lehui, Dan Zhao, Wing-Hong Chan, Martin MF Choi, and Hung-Wing Li. "Inhibition of beta 1–40 amyloid fibrillation with N-acetyl-l-cysteine capped quantum dots." *Biomaterials* 31, no. 1 (2010): 91-98.

[29] Sievers, Stuart A., John Karanicolas, Howard W. Chang, Anni Zhao, Lin Jiang, Onofrio Zirafi, Jason T. Stevens, Jan Münch, David Baker, and David Eisenberg. "Structure-based design of non-natural amino-acid inhibitors of amyloid fibril formation." *Nature* 475, no. 7354 (2011): 96-100.

[30] Gordon, David J., Kimberly L. Sciarretta, and Stephen C. Meredith. "Inhibition of β-amyloid (40) fibrillogenesis and disassembly of β-amyloid (40) fibrils by short β-amyloid congeners containing N-methyl amino acids at alternate residues." *Biochemistry* 40, no. 28 (2001): 8237-8245.

[31] Wang, Steven S-S., Shang-Wei Chou, Kuan-Nan Liu, and Chia-Hung Wu. "Effects of glutathione on amyloid fibrillation of hen egg-white lysozyme." *International journal of biological macromolecules* 45, no. 4 (2009): 321-329.

[32] Dubey, Kriti, Bibin G. Anand, Rahul Badhwar, Ganesh Bagler, P. N. Navya, Hemant Kumar Daima, and Karunakar Kar. "Tyrosine-and tryptophan-coated gold nanoparticles inhibit amyloid aggregation of insulin." *Amino acids* 47, no. 12 (2015): 2551-2560

[33] Shafai, Ghazal S., Sharan Shetty, Sailaja Krishnamurty, Vaishali Shah, and D. G. Kanhere. "Density functional investigation of the interaction of acetone with small gold clusters." *The Journal of chemical physics* 126, no. 1 (2007): 014704.

[34] De Jong, Wim H., and Paul JA Borm. "Drug delivery and nanoparticles: applications and hazards." *International journal of nanomedicine* 3, no. 2 (2008): 133.

[35] Aili, Daniel, Karin Enander, Johan Rydberg, Irina Nesterenko, Fredrik Björefors, Lars Baltzer, and Bo Liedberg. "Folding induced assembly of polypeptide decorated gold nanoparticles." *Journal of the American Chemical Society* 130, no. 17 (2008): 5780-5788.

[36] Sperling, Ralph A., Pilar Rivera Gil, Feng Zhang, Marco Zanella, and Wolfgang J. Parak. "Biological applications of gold nanoparticles." *Chemical Society Reviews* 37, no. 9 (2008): 1896-1908.

[37] Wangoo, Nishima, C. Raman Suri, and G. Shekhawat. "Interaction of gold nanoparticles with protein: a spectroscopic study to monitor protein conformational changes." *Applied Physics Letters* 92, no. 13 (2008): 133104.

[38] Álvarez, Yanina D., Jonathan A. Fauerbach, Jésica V. Pellegrotti, Thomas M. Jovin, Elizabeth A. Jares-Erijman, and Fernando D. Stefani. "Influence of gold nanoparticles on the kinetics of α-synuclein aggregation." *Nano letters* 13, no. 12 (2013): 6156-6163.

[39] Shiraki, Kentaro, Motonori Kudou, Shinsuke Fujiwara, Tadayuki Imanaka, and Masahiro Takagi. "Biophysical effect of amino acids on the prevention of protein aggregation." *Journal of biochemistry* 132, no. 4 (2002): 591-595.

[40] Selvakannan, P. R., Saikat Mandal, Sumant Phadtare, Anand Gole, Renu Pasricha, S. D. Adyanthaya, and Murali Sastry. "Water-dispersible tryptophan-protected gold nanoparticles prepared by the spontaneous reduction of aqueous chloroaurate ions by the amino acid." *Journal of colloid and interface science* 269, no. 1 (2004): 97-102.

[41] Zare, D., A. Akbarzadeh, and N. Bararpour. "Synthesis and functionalization of gold nanoparticles by using of poly functional amino acids." *International Journal of Nanoscience and Nanotechnology* 6, no. 4 (2010): 223-230.

[42] Wangoo, Nishima, K. K. Bhasin, S. K. Mehta, and C. Raman Suri. "Synthesis and capping of water-dispersed gold nanoparticles by an amino acid: bioconjugation and binding studies." *Journal of colloid and interface science* 323, no. 2 (2008): 247-254.

[43] Cai, Huanxin, and Ping Yao. "Gold nanoparticles with different amino acid surfaces: Serum albumin adsorption, intracellular uptake and cytotoxicity." *Colloids and Surfaces B: Biointerfaces* 123 (2014): 900-906.

[44] Samuel, Dharmaraj, Gopal Ganesh, Pey- Wen Yang, Mei- Ming Chang, Sue- Lein Wang, Kuo- Chu Hwang, Chin Yu et al. "Proline inhibits aggregation during protein refolding." *Protein Science* 9, no. 2 (2000): 344-352.

[45] Seeliger, Janine, Kathrin Estel, Nelli Erwin, and Roland Winter. "Cosolvent effects on the fibrillation reaction of human IAPP." *Physical Chemistry Chemical Physics* 15, no. 23 (2013): 8902-8907.

[46] Srinivas, V., and D. Balasubramanian. "Proline is a protein-compatible hydrotrope." *Langmuir* 11, no. 7 (1995): 2830-2833.

[47] Schobert, Brigitte, and Harald Tschesche. "Unusual solution properties of proline and its interaction with proteins." *Biochimica et Biophysica Acta (BBA)-General Subjects* 541, no. 2 (1978): 270-277.

[48] Choudhary, Sinjan, Shreyada N. Save, Nand Kishore, and Ramakrishna V. Hosur. "Synergistic Inhibition of Protein Fibrillation by Proline and Sorbitol: Biophysical Investigations." *PloS one* 11, no. 11 (2016): e0166487.

[49] Li, Shun-Cheng, Natalie K. Goto, Karen A. Williams, and Charles M. Deber. "Alpha-helical, but not beta-sheet, propensity of proline is determined by peptide environment." *Proceedings of the National Academy of Sciences* 93, no. 13 (1996): 6676-6681.

[50] Moriarty, Daniel F., and Daniel P. Raleigh. "Effects of sequential proline substitutions on amyloid formation by human amylin20-29." *Biochemistry* 38, no. 6 (1999): 1811-1818.

[51] Rai, Sandhya, NV Suresh Kumar, and Harjinder Singh. "A theoretical study on interaction of proline with gold cluster." *Bulletin of Materials Science* 35, no. 3 (2012): 291-295.

[52] Swaminathan, Rajaram, Vijay Kumar Ravi, Satish Kumar, Mattaparthi Venkata Satish Kumar, and Nividh Chandra. "Lysozyme: a model protein for amyloid research." *Adv Protein Chem Struct Biol* 84, no. 1 (2011): 63-111

[53] Pertinhez, Thelma A., Mario Bouchard, Esther J. Tomlinson, Rachel Wain, Stuart J. Ferguson, Christopher M. Dobson, and Lorna J. Smith. "Amyloid fibril formation by a helical cytochrome." *FEBS letters* 495, no. 3 (2001): 184-186

[54] Turkevich, John, Peter Cooper Stevenson, and James Hillier. "A study of the nucleation and growth processes in the synthesis of colloidal gold." *Discussions of the Faraday Society* 11 (1951): 55-75.

[55] Kimling, J., M. Maier, B. Okenve, Vassilios Kotaidis, H. Ballot, and Anton Plech. "Turkevich method for gold nanoparticle synthesis revisited." *The Journal of Physical Chemistry B* 110, no. 32 (2006): 15700-15707.

[56] Majzik, A., L. Fülöp, E. Csapó, F. Bogár, T. Martinek, B. Penke, G. Bíró, and Imre Dékány. "Functionalization of gold nanoparticles with amino acid, β-amyloid peptides and fragment." *Colloids and Surfaces B: Biointerfaces* 81, no. 1 (2010): 235-241.

[57] Liu, Kuan-Nan, Chia-Min Lai, Yi-Ting Lee, Sung-Ning Wang, Rita P-Y. Chen, Jeng-Shiung Jan, Hwai-Shen Liu, and Steven S-S. Wang. "Curcumin's pre-incubation temperature affects its inhibitory potency toward amyloid fibrillation and fibril-nduced

cytotoxicity of lysozyme." *Biochimica et Biophysica Acta (BBA)-General Subjects* 1820, no. 11 (2012): 1774-1786.

[58] de Groot, Natalia S., and Salvador Ventura. "Amyloid fibril formation by bovine cytochrome c." *Journal of Spectroscopy* 19, no. 4 (2005): 199-205.

[59] Khurana, Ritu, Chris Coleman, Cristian Ionescu-Zanetti, Sue A. Carter, Vinay Krishna, Rajesh K. Grover, Raja Roy, and Shashi Singh. "Mechanism of thioflavin T binding to amyloid fibrils." *Journal of structural biology* 151, no. 3 (2005): 229-238.

[60] Lee, C. H. "1-anilinonaphthalene-8-sulfonate (ANS); a versatile fluorescent probe from protein folding study to drug design." *BioWave* 12, no. 6 (2010): 1.

[61] Ghosh, Sudeshna, Nitin K. Pandey, and Swagata Dasgupta. "(−)-Epicatechin gallate prevents alkali-salt mediated fibrillogenesis of hen egg white lysozyme." *International journal of biological macromolecules* 54 (2013): 90-98.

[62] Pras, M., M. Schubert, D. Zucker-Franklin, A. Rimon, and E. C. Franklin. "The characterization of soluble amyloid prepared in water." *Journal of Clinical Investigation* 47, no. 4 (1968): 924.

[63] Garbuzynskiy, Sergiy O., Michail Yu Lobanov, and Oxana V. Galzitskaya. "FoldAmyloid: a method of prediction of amyloidogenic regions from protein sequence." *Bioinformatics* 26, no. 3 (2010): 326-332.

[64] Schneidman-Duhovny, Dina, Yuval Inbar, Ruth Nussinov, and Haim J. Wolfson. "PatchDock and SymmDock: servers for rigid and symmetric docking." *Nucleic acids research* 33, no. suppl 2 (2005): W363-W367.

[65] Andrusier, Nelly, Ruth Nussinov, and Haim J. Wolfson. "FireDock: fast interaction refinement in molecular docking." *Proteins: Structure, Function, and Bioinformatics* 69, no. 1 (2007): 139-159.

[66] Wallace, Andrew C., Roman A. Laskowski, and Janet M. Thornton. "LIGPLOT: a program to generate schematic diagrams of protein-ligand interactions." *Protein engineering* 8, no. 2 (1995): 127-134.

[67] Mu, Xiaoyu, Li Qi, Ping Dong, Juan Qiao, Jian Hou, Zongxiu Nie, and Huimin Ma. "Facile one-pot synthesis of l-proline-stabilized fluorescent gold nanoclusters and its application as sensing probes for serum iron." *Biosensors and Bioelectronics* 49 (2013): 249-255.

[68] Das T, Kolli V, Karmakar S, Sarkar N. "Functionalisation of Polyvinylpyrrolidone on Gold Nanoparticles Enhances Its Anti-Amyloidogenic Propensity towards Hen Egg White Lysozyme." *Biomedicines* 5, no. 2 (2017): 19.